Distributed Energy Resource and Network Expansion Planning of a CCHP based Active Microgrid Considering Demand Response Programs

Farid Varasteh[a], Mehrdad Setayesh Nazar[b], Alireza Heidari[c], Miadreza Shafie-khah[d], and João P. S. Catalão[e,f,g*]

[a] *Faculty of Mechanical and Energy Engineering, Shahid Beheshti University, AC., Tehran, Iran*

[b] *Faculty of Electrical Engineering, Shahid Beheshti University, AC., Tehran, Iran*

[c] *School of Electrical Engineering and Telecommunications, The University of New South Wales, Sydney, Australia*

[d] *INESC TEC, 4200-465 Porto, Portugal*

[e] *Faculty of Engineering of the University of Porto and INESC TEC, 4200-465 Porto, Portugal*

[f] *C-MAST, University of Beira Interior, 6201-001 Covilhã, Portugal*

[g] *INESC-ID, Instituto Superior Técnico, University of Lisbon, 1049-001 Lisbon, Portugal*

**corresponding author (catalao@ubi.pt) at Faculty of Engineering of the University of Porto and INESC TEC*

Abstract

This paper addresses the network expansion planning of an active microgrid that utilizes Distributed Energy Resources (DERs). The microgrid uses Combined Cooling, Heating and Power (CCHP) systems with their heating and cooling network. The proposed method uses a bi-level iterative optimization algorithm for optimal expansion and operational planning of the microgrid that consists of different zones, and each zone can transact electricity with the upward utility. The transaction of electricity with the upward utility can be performed based on demand response programs that consist of the time-of-use program and/or direct load control. DERs are CHPs, small wind turbines, photovoltaic systems, electric and cooling storage, gas fired boilers and absorption and compression chillers are used to supply different zones' electrical, heating, and cooling loads. The proposed model minimizes the system's investment, operation, interruption and environmental costs; meanwhile, it maximizes electricity export revenues and the reliability of the system. The proposed method is applied to a real building complex and five different scenarios are considered to evaluate the impact of different energy supply configurations and operational paradigm on the investment and operational costs. The effectiveness of the introduced algorithm has been assessed. The implementation of the proposed algorithm reduces the aggregated investment and operational costs of the test system in about 54.7% with respect to the custom expansion planning method.

Keywords**:** District heating; District cooling; Active microgrid; Demand response.

Nomenclature

Abbreviation

AC	Alternative Current.
ACH	Absorption Chiller.
CCH	Compression Chiller.
CHP	Combined Heating and Power.
CCHP	Combined Cooling, Heating and Power.
CSS	Cool Storage systems.
DC	Direct Current.
DCS	District Cooling System.
DER	Distributed Energy Resource.
DERNEP	Distributed Energy Resource and Networks Expansion Planning.
DHS	District Heating System.
DHCN	District Heating and Cooling Network.
DLC	Direct Load Control.
DRP	Demand Response Program.
ESS	Electrical Storage System.
GA	Genetic Algorithm.
HCL	Heating and Cooling Load.
LSP	Load Shedding Procedure.
MG	MicroGrid.
MILP	Mix Integer Linear Programming.
MINLP	Mixed Integer Non-Linear Programming.
MUs	Monetary Units.
MMUs	Million MUs.
NOE	Number of Optimization Equations
OPF	Optimal Power Flow
PVA	Solar Photovoltaic Array.
SCOPF	Security Constrained Optimal Power Flow.
SWT	Small Wind Turbine.
SOC	State of Charge
TOU	Time-of-Use.

Index and Sets

a	CHP installation site index.
b	CHP capacity selection alternatives index.
d	CHP time of operation index.
a'	ESS installation site index.
b'	ESS capacity selection alternatives index.
d'	ESS time of operation index.
a''	CSS installation site index.
b''	CSS capacity selection alternatives index.
d''	CSS time of operation index.
e	Boiler installation site index.
f	Boiler capacity selection alternatives index.
g	Boiler time of operation index.
i	Year of planning index.
j	Zone of MG index.
k'	ACH time of operation index.

i'	ACH installation site index.
j'	ACH capacity selection alternatives index.
k''	CCH time of operation index.
i''	CCH installation site index.
j''	CCH capacity selection alternatives index.
m	Upward utility transformer site and/or CHP installation site index.
n	Load site index.
m'	DHC installation site index.
n'	HCL site index.
q	PVA installation site index.
q'	SWT installation site index.
t	Time index.
X	CCH and/or ACH index.
α	Electric system contingency index.

Parameters

A^{PVA}	Area of photovoltaic array (m^2).
ACH_Site	Absorption chiller site.
$ACHC$	Absorption chiller capacity selection alternatives.
$Boiler\_Site$	Boiler site.
B_{Sell}	Benefit of energy sold to upward utility (MUs).
B_{DRP}	Benefit of DRPs (MUs).
BC	Boiler capacity selection alternatives.
C_{CHP}	Investment, operational, emission and maintenance costs of CHP unit (MUs).
C_{Feeder}	Investment costs of electric feeder (MUs).
C_{Pipe_DCS}	Investment costs of district cooling system pipe (MUs).
C_{Pipe_DHS}	Investment costs of district heating system pipe (MUs).
C_{ACH}	Aggregated investment, operational and maintenance costs of absorption chiller (MUs).
C_{CCH}	Aggregated investment, operational and maintenance costs of compression chiller (MUs).
C_{PVA}	Aggregated investment and maintenance costs of photovoltaic array (MUs).
C_{SW}	Aggregated investment and maintenance costs of switching device (MUs).
C_{SWT}	Aggregated investment and maintenance costs of small wind turbine (MUs).
C_{ESS}	Aggregated investment, operational and maintenance costs of electricity storage (MUs).
C_{CSS}	Aggregated investment, operational and maintenance costs of cooling storage (MUs).
C_{Boiler}	Aggregated investment, operational, emission and maintenance costs of boiler (MUs).
$C_{Purchase}$	Cost of electricity purchased from upward utility (MUs).
C_{Invest}	Investment cost (MUs).
C_{Op}	Operational cost (MUs/MWh).
C_{M}	Maintenance cost (MUs/MWh).
C_{EM}	Emission cost (MUs/kg).

Cap^{ESS}	Capacity of electricity storage (kW).
Cap^{CSS}	Capacity of cooling storage (kW_c).
$CCHC$	Compression chiller capacity selection alternatives.
CCH_Site	Compression chiller site.
COP_{ACH}	Coefficient of performance of absorption chiller.
COP_{CCH}	Coefficient of performance of compression chiller.
C_{Inv}^{PVA}	Investment cost of photovoltaic array (MUs/MW).
C_{Inv}^{CSS}	Investment cost of cooling storage (MUs/MWh).
C_{Inv}^{ESS}	Investment cost of electricity storage (MUs/MWh).
$C_{Capacity}^{Feeder}$	Capacity dependent cost of electric feeder (MUs/kW).
Cap^{Feeder}	Capacity of electric feeder (kW).
C_{leng}^{Feeder}	Length dependent cost of electric feeder (MUs/m).
$C_{Capacity}^{DH}$	Capacity dependent cost of district heating system pipe (MUs/m.MW).
Cap^{DH}	Capacity of district heating system pipe (MW).
C_{leng}^{DH}	Length dependent cost of district heating system pipe (MUs/m).
$C_{Capacity}^{DC}$	Capacity dependent cost of district cooling system pipe (MUs/m.MW).
Cap^{DC}	Capacity of district cooling system pipe (MW).
C_{leng}^{DC}	Length dependent cost of district cooling system pipe (MUs/m).
C_{IC}	Total interruption cost.
CHP_Site	CHP installation alternative site.
$CHPC$	CHP capacity selection alternatives.
CDF	Composite damage function (MU/MWh).
$CSSC$	Cool storage capacity selection alternatives.
CSS_Site	Cool storage installation alternative site.
DHC_Site	District heating and cooling site.
$ESSC$	Electricity storage capacity selection alternatives.
ESS_Site	Electricity storage installation alternative site.
EM_{CO_2}	CO2 emission (ton/yr).
EM_{SO_2}	SO2 emission (kg/yr).
EM_{NO_X}	NOX emission (kg/yr).
EMC_{CO_2}	CO2 emission penalty cost (MUs/ton.yr)
EMC_{SO_2}	SO2 emission penalty cost (MUs/kg.yr)
EMC_{NO_X}	NOX emission penalty cost (MUs/kg.yr)
HCL_Site	Heating and cooling load site.
I	Solar irradiation (kW/m^2).
L	Distance between energy carrier generation site and load site (m).

L_P	Weighted decibels (dBA).
$Load\_Site$	Electric load site.
$Ncont$	Number of zone's electric system contingencies.
P^{CCH}	Electric power consumption of compression chiller (kW).
P_{shed}	Shed electrical energy (kW).
PDC^{ESS}	Electric power discharge of electricity storage (kW).
P^{MG}	Electric power of microgrid (kW).
P^{DRP}	Demand response program electric power generation/reduction (kW).
P^{Load}	Electric power of electric load (kW).
P^{PVA}	Electric power generated by photovoltaic array (kW).
P^{ESS}	Electric power delivered by electricity storage (kW).
$P_{Critical}^{Load}$	Critical electrical load (kW).
$P_{Deferrable}^{Load}$	Deferrable electrical load (kW).
$P_{Controllable}^{Load}$	Controllable electrical load (kW).
P^{SWT}	Electric power generated by SWT.
ΔP^{TOU}	Electric power injection/withdrawal changed for time-of-use program (kW).
ΔP^{DLC}	Electric power withdrawal changed for DLC program (kW).
PVA_Site	Photovoltaic array site.
Q^{Load}	Thermal load (kW_{th}).
Q^{ACH}	CHP thermal power delivered to absorption chiller (kW_{th}).
Q^{CHP}	CHP thermal power output (kW_{th}).
Q^{Loss}	Loss of thermal power (kW_{th}).
Q^{Flow}	Thermal power flow in district heating system pipe (kW_{th}).
R^{DHC}	Radius of district heating or cooling pipe (m).
R^{CCH}	Cooling power generated by compression chiller (kW_c).
R^{Load}	Cooling load (kW_c).
R^{ACH}	Cooling power generated by absorption chiller (kW_c).
R^{Loss}	Loss of cooling power (kW_c).
R^{CSS}	Cooling power delivered by cooling storage (kW_c).
R^{Flow}	Cooling power flow in district cooling system pipe (kW_c).
RDC^{CSS}	Cooling power discharge of cooling storage (kW_c).
RC^{CSS}	Cool storage charging power (kW_c).
R^{SWT}	Small wind turbine blade radius (m).
SWT_Site	Small wind turbine site.

Variables

T_{ACH}	Aggregated duration of absorption chiller operation.
T_{Boiler}	Aggregated duration of boiler operation.
T_{CCH}	Aggregated duration of compression chiller operation.
T_{ESS}	Aggregated duration of ESS operation.
T_{CSS}	Aggregated duration of CSS operation.
T_{CHP}	Aggregated duration of CHP operation.
t_0	Outside air temperature (°C).
$Trans \cup CHP\_Site$	The set of upward utility transformer and CHP sites.
X^{CSS}	Binary variable of cooling storage discharge; equals 1 if cooling storage is discharged.
X^{ESS}	Binary variable of electricity storage discharge; equals 1 if electricity storage is discharged.
Y^{CSS}	Binary variable of cooling storage charge; equals 1 if cooling storage is charged.
Y^{ESS}	Binary variable of electricity storage charge; equals 1 if electricity storage is charged.
W	Weight factor.
σ	Present worth factor.
γ	Probability of contingency.
φ	Binary decision variable of device installation (equals to 1 if device is installed).
τ	Duration of device operation.
$\chi_{\max}$	Maximum velocity of energy carrier in pipe (m/s).
$\xi^{Elect}_{Purchased}$	Electricity purchasing price that is purchased from upward utility (MUs/kWh).
ξ^{Elect}_{Sell}	Electricity selling price that is sold to upward utility (MUs/kWh).
ξ^{Elect}_{DLC}	Energy cost of DLC program (MUs/kWh).
ϑ	Maximum discharge coefficient of cooling storage.
ϖ	Maximum discharge coefficient of electricity storage.
$\alpha'^{th}_{CHP}, \beta'^{th}_{CHP}, \gamma'^{th}_{CHP}$	Coefficient of heat-power feasible region for CHP unit.
Ω	Small wind turbine blade angular velocity [rad/s].
η	Photovoltaic array conversion efficiency.
ρ_{water}	Water density (kg/m3).
$\Delta\theta_{(input-output)}$	Temperature difference of input/output water (°C).
ζ	Specific heat capacity.
v^{Wind}_c	Small wind turbine cut-in wind velocity.
v^{Wind}_f	Small wind turbine cut-off wind speed.

1. Introduction

The Combined Cooling, Heating and Power (CCHP) system contributes to increasing the interdependencies of cooling, heating and electricity systems and the efficiency of the energy systems. CCHP-based systems can be utilized by MicroGrids (MGs) in either the grid-connected or island mode of operation [1].

The CCHP-based MG's electric loads can be supplied through the utility grid and it can participate in utility's Demand Response Programs (DRP) by reducing its withdrawal from the grid and increasing the power generation of its electricity generation systems. Thus, the MG may behave as an Active MG (AMG) that transacts electricity with upward utility [2]. However, based on the AMGs' cooling, heating and electric load characteristics and/or systems constraints, the AMG can be segmented into different internal zones that each zone can transact cooling and heating energy with others through District Heating and Cooling Network (DHCN) [3].

Chicco et al. [4] outlined the aspects of the distributed multi-generation system framework based on a discrete time snapshot and a black-box approach. This reference summarizes that the designed problem for steady-state conditions can be used to model the system's performance.

Distributed Energy Resource and Networks Expansion Planning (DERNEP) problem of an AMG consists of determining the cooling, heating and electric generation, network and energy storage device location, capacity, and the time of installation depending on the load growth, reliability criteria, characteristics of devices and cost-benefit analysis [4]. However, the reliability aspects of the planning procedure must be explored by the simulation of electric system contingencies based on the fact that each of the electric system contingency may generate new state spaces. The electric system contingency can lead to high nonlinearity and non-convexity of the system's model. The optimization problem has a great non-convex discrete state space and its solution algorithm must have the ability to effectively model the nonlinearity and non-convexity of the system's state space and the dynamic coupling constraints of the electric, heating and cooling systems.

Over recent years, different aspects of DERNEP have been studied and the literature can be categorized into the following groups. The first category developed models for device specification, static and dynamic methods of capacity expansion, long-term/short-term energy management and performance evaluation. The second category proposes solution techniques that determine the global optimum of the first category problems. The third category introduces new conceptual ideas in the DERNEP paradigms.

Based on the first category of researches, many papers have presented for optimal design and operation of CCHP-based systems that solve planning problem by using Mix Integer Linear Programming (MILP), nonlinear programming, Mix Integer Non-Linear Programming (MINLP), heuristic and meta-heuristic methods [5,6].

Lozano et al. [7] presented a cost-based MILP model of CCHP design that minimizes the total annual planning cost consists of investment and operational costs. Ref. [7] considers the legal constraints and the model is assessed by a case study for 5000 apartments in Spain. It concludes that the self-consumption obligation is a barrier to a wider use of CCHP systems in the Spanish residential sector. Carvalho et al. [8] introduced a simple MILP model for optimal design and operation of a real district heating system utilizing linearization

techniques. The optimal configuration of tri-generation systems is obtained by different environmental criteria that the possibility for sale of electricity to the upward electric grid is considered.

Zheng et al. [9] presented a robust MINLP model that optimizes the configuration, sizing and operation of CCHP systems taking into account the time-dependent demands and the model was applied for a pilot zone in urban China. The model was assessed for four scenarios, namely baseline, low energy, low Carbon dioxide (CO_2) emissions, and integrated scenarios. The result shows that energy saving and CO_2 emissions are achievable by the installation of Solar Photovoltaic Arrays (PVAs), CCHPs and storage systems. Zelin Li et al. [10] proposed a multi-objective optimization model for CCHP system, the performances of different feed-in tariffs were evaluated, and the annual costs and carbon emissions were compared. The proposed optimization uses the analytic hierarchy process to determine the objective functions and the model is analyzed with different feed-in tariffs for buildings in Sino-Singapore.

Miao Li et al. [11] presented a model to explore the benefits of gas fired CCHP systems based on economic, energetic and environmental criteria using fuzzy selection method. Results show that: 1) CCHP systems reduce the annual costs compared with the reference system; 2) CCHP systems have no economic merits for residential systems; 3) The CCHP systems decrease pollutant emissions.

Liwei Ju et al. [12] used a multi-objective optimization model that contained energy rate, operation cost, CO_2 emission reductions for Distributed Energy Resource (DER)-CCHP based system. The model optimizes daily operational strategy of three subsystems that each subsystem consists of CCHP, electric and heating systems. The results show that the DERs CCHP system highly reduces CO_2 emission.

Sakawa et al. [13] explored the operational planning problem of DHC using binary MILP algorithm. The results show that it is difficult to obtain exact optimal solutions of DHC planning. Thus, a Genetic Algorithm (GA) is proposed for 0-1 MILP problem, and it concludes that GA is more efficient than the branch-and-bound method for different scenarios.

Weber et al. [14] introduced an optimization procedure based on MILP technique that explored the optimal combinations of technologies for supplying of a small-town district energy system. It performs a sensitivity analysis to determine the optimal mix of technologies and it minimizes the CO_2 environmental emissions. The most important shortcomings of the presented models in these references are lack of consideration of the electric system contingencies and non-linear Security Constrained Optimal Power Flow (SCOPF) model of the electric system.

Ameri et al [15] presented a MILP model for optimal planning of CCHP/DHCN for a residential district considering four planning scenarios without considering of Electrical Storage Systems (ESSs) and Cool Storage systems (CSSs). Soderman et al. [16] proposed a mixed integer optimization algorithm that determines the optimal layout and capacity of the system and minimizes the aggregated investment and operational costs. The model considers

a different combination of Combined Heating and Power (CHP), boiler and wind turbines for finding the optimal layout of the system. Mehleri et al. [17] presented an optimal planning algorithm that uses a MILP formulation to minimize energy costs. The presented method considers climate and tariffs constraints and it determines the parameters of DER systems, district heating pipelines and heating storages. Bracco et al. [18] explored a multi-objective MILP optimization model that optimizes capital and operating costs of combined heating and power generation systems. The proposed model was implemented in the city of Arenzani in Italy.

Boloukat et al. [19] presented an algorithm for expansion planning of microgrid considering DERs. The proposed algorithm maximizes profit and reliability, while it minimizes investment and operation costs. Hemmati et al. [20] introduced a two-level planning algorithm. The algorithm determines the optimal location and size of devices and it considers DERs. Refs. [15-20] do not consider the SCOPF model and contingencies of the electric system.

The integrated energy resource and network expansion planning of CCHP-based AMG optimization algorithm considering DRPs, Small Wind Turbines (SWTs), PVAs, ESSs, and CSSs are less frequent in the previous researches. Table 1 shows the comparison of the proposed DERNEP model with the other researches.

The present research proposes a DERNEP framework that uses the MINLP model. The main contributions of this paper can be summarized as follows:

- It represents an integrated model for DERNEP considering renewable energy resources, electricity and cooling storage systems, CCHPs and DHCNs.
- The proposed formulation explores the optimum expansion planning and operation scheduling of energy resources for minimizing the microgrid costs and maximizing the system's reliability,
- The proposed bi-level algorithm investigates the adequacy of system resources in the normal and contingent operational conditions based on the fact that the electric system contingency can lead to high nonlinearity and non-convexity of the system's model.
- The SCOPF optimization problem explores the detailed optimal operation of cooling, heating and electric systems and it investigates the adequacy of system resources for the most important loads based on the 'N-1' concept. The SCOPF problem simulates the outage of one component of the electric system and it tries to find the optimal coordination of other system resources after the switching of switching devices.
- The optimization problem has a great non-convex discrete state space and the proposed solution algorithm has the ability to model the nonlinearity and non-convexity of the state space and the dynamic coupling constraints of the electric, heating and cooling systems.

Table 1: Comparison of proposed DERNEP with other researches.

References		[5]	[7]	[8]	[9]	[10]	[11]	[12]	[13]	[14]	[15]	[16]	[17]	[18]	[19]	[20]	Proposed Approach
Method	MILP	×	✓	✓	×	×	×	×	×	✓	✓	✓	✓	✓	✓	×	×
	MINLP	✓	×	×	✓	×	×	×	×	×	×	×	×	×	×	×	✓
	Heuristic	×	×	×	×	✓	✓	✓	✓	×	×	×	×	×	×	✓	×
Objective Function	Revenue	×	×	✓	×	×	×	×	×	×	✓	×	✓	✓	×	×	✓
	Generation Cost	✓	✓	✓	✓	✓	✓	✓	✓	✓	✓	✓	✓	✓	✓	✓	✓
	Storage Cost	×	✓	×	✓	×	×	✓	×	✓	×	✓	✓	×	✓	✓	✓
	Electric System Contingency	×	×	×	×	×	×	×	×	×	×	×	×	×	×	×	✓
	SCOPF model	×	×	×	×	×	×	×	×	×	×	×	×	×	×	×	✓
	Emission	×	×	✓	✓	✓	✓	✓	×	✓	✓	×	×	✓	×	×	✓
	TOU	×	×	×	✓	✓	×	×	×	×	×	×	✓	×	×	×	✓
	DLC	×	×	×	×	×	×	×	×	×	×	×	×	×	×	×	✓
	SWT	×	×	×	×	×	×	✓	×	×	×	×	×	×	✓	✓	✓
	PVA	×	×	×	✓	×	×	✓	×	✓	✓	×	✓	×	✓	✓	✓
Nonlinear feasible operating region of CHP unit		✓	✓	✓	✓	×	×	✓	×	✓	✓	✓	✓	✓	×	×	✓
Storage System	EES	×	×	×	✓	×	×	×	×	×	×	×	✓	×	✓	✓	✓
	CSS	×	✓	×	✓	×	×	×	×	×	×	×	×	×	×	×	✓
Constraints of AMG Zones		×	×	×	×	×	×	×	×	×	×	×	×	×	×	×	✓
Grid Connected		✓	✓	✓	✓	✓	✓	✓	✓	✓	✓	✓	✓	✓	✓	✓	✓
Optimal operation coordination of zones		×	×	×	×	×	×	×	×	×	×	×	×	×	×	×	✓
Expansion Planning		×	×	×	×	×	×	×	×	×	×	×	×	×	✓	✓	✓

The following sections of this paper are organized as follows: The modelling and formulation of the DERNEP problem are introduced in Section 2. In Section 3, the solution algorithm is presented. In section 4, the numerical results for different scenarios are presented. Finally, the conclusions are included in Section 5.

2. Problem Modeling and Formulation

The AMG owner utilizes CHP-based CCHP systems to supply its cooling, heating and electricity. As mentioned earlier, the AMG is segmented into different internal zones that each zone is equipped with different energy resources consists of CCHPs, compression chillers, gas –fired boilers, PVAs, SWTs, ESSs, and CSSs as shown in Fig. 1. Each zone can transact cooling and heating energy with other zones through DHCN. Further, the electricity surplus of each zone can be sold to the upward utility grid. The AMG site is composed of several buildings blocks and the AMG expansion planning consists of the construction of

new buildings in different zones. The proposed algorithm can consider the optimal expansion planning and operation of aggregated zones and/or individual zones based on the fact that the optimal DERNEP of an individual zone may improve the zonal self-sufficiency of energy supply and the flexibility of their responses to the upward utility's DRPs.

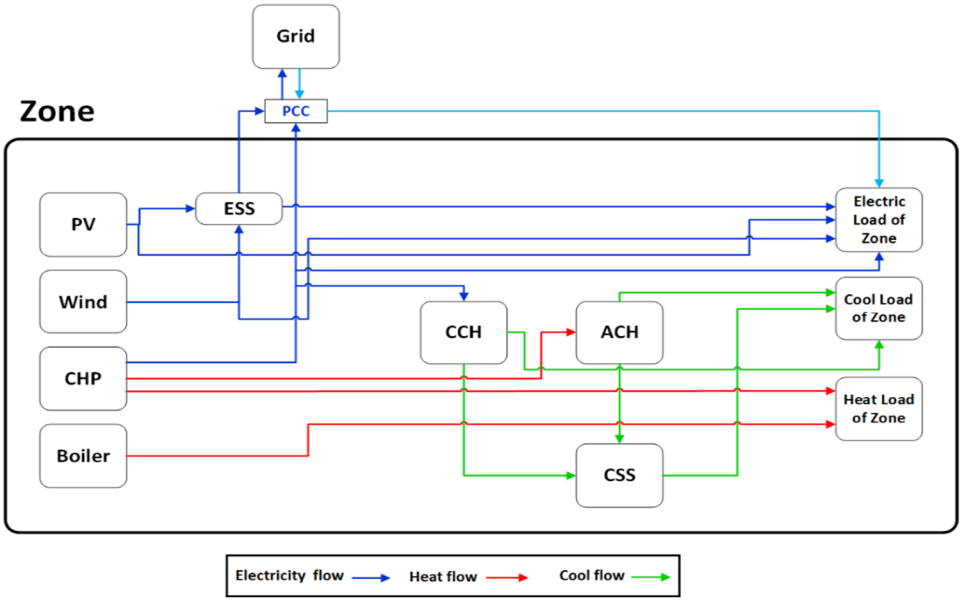

Fig. 1. The AMG zones energy resources and storages and electric, heating and cooling loads.

The DERNEP is logical in light of AMG cooling, heating and electric demands and system optimal operation. The DERNEP should simultaneously optimize the investment and estimated hourly energy carriers dispatch problems [21]. The described DERNEP problem has a large state space that involves thousands of variables in expansion planning horizon. The electricity, heating and cooling load data, renewable and conventional energy resources investment and operational data and DRP highly increase the state space of the DERNEP problem. Thus, the trade-off between accuracy and computational burden is made to derive the best DERNEP solution algorithm without oversimplifying the expansion planning process. Hence, the authors try to find the reasonable trade-off between solution quality and acceptable calculation time.

2.1. First Stage Problem Formulation

An optimal DERNEP must locate the minimized total costs solution where the total cost consists of the total investment costs, the aggregated operation costs and the AMG's electricity purchasing and selling costs.

The objective function of DERNEP problem can be written as (1):

$$Min\ \mathbf{Z} = \sum_{i}^{Nyear} \sum_{j}^{Nzone} \left(\begin{array}{l} (C_{CHP}\ .\varphi_{ij}^{CHP} + C_{Feeder}.\varphi_{ij}^{Feeder} + C_{Pipe\_DCS}.\varphi_{ij}^{Pipe\_DCS} + C_{Pipe\_DHS}.\varphi_{ij}^{Pipe\_DHS} + \\ C_{ACH}\ .\varphi_{ij}^{ACH} + C_{CCH}.\varphi_{ij}^{CCH} + C_{PVA}.\varphi_{ij}^{PVA} + C_{SWT}.\varphi_{ij}^{SWT} + C_{ESS}.\varphi_{ij}^{ESS} \\ + C_{CSS}.\varphi_{ij}^{CSS} + C_{Boiler}.\varphi_{ij}^{Boiler} + C_{SW}.\varphi_{ij}^{SW}) + C_{IC} + C_{Purchase} - B_{Sell} - B_{DRP} \end{array} \right) \quad (1)$$

The objective function can be decomposed into five groups: 1) the investment plus aggregated operation costs of: CHP (C_{CHP}), electric feeder (C_{Feeder}), District Cooling System (DCS) pipe (C_{Pipe_DCS}), District Heating System (DHS) pipe (C_{Pipe_DHS}), Absorption CHiller (ACH) (C_{ACH}), Compression CHiller (CCH) (C_{CCH}), PVA (C_{PVA}), SWT (C_{SWT}), ESS (C_{ESS}), CSS (C_{CSS}), boiler (C_{Boiler}), and switching device (C_{SW}), 2) The interruption cost of electric system contingency (C_{IC}), 3) the costs of energy purchased from upward utility $(C_{Purchase})$, 4) the benefits of energy sold to utility (B_{Sell}), and 5) the benefits of DRPs (B_{DRP}). The second, third, fourth and fifth group of objective functions are calculated at the second stage problem. The CHP, boiler, ACH, CCH, ESS, and CSS investment cost (C_{Invest}) and aggregated operation costs consist of annualized fixed costs and variable costs. The variable costs are modelled as a function of operation time and their corresponding operation cost (C_{Op}), maintenance cost (C_M) and emissions cost (C_{EM}). Thus, the CHP, boiler, ACH, CCH, ESS, and CSS investment and aggregated operation costs can be written as (2-7):

$$C_{CHP} = \sigma. \sum_{a\in CHP\_Site} \sum_{b\in CHPC} (C^{CHP}_{Invest}{}_{ab} + \sum_{d\in T_{CHP}} \tau_d.(C^{CHP}_{Op}{}_{abd} + C^{CHP}_{M}{}_{abd} + C^{CHP}_{EM}{}_{abd})) \quad (2)$$

$$C^{CHP}_{EM\ abd} = EM^{CHP}_{CO_2}{}_{abd}.EMC_{CO_2}{}_{abd} + EM^{CHP}_{SO_2}{}_{abd}.EMC_{SO_2}{}_{abd} + EM^{CHP}_{NO_X}{}_{abd}.EMC_{NO_X}{}_{abd} \quad (3)$$

$$C_{Boiler} = \sigma. \sum_{e\in Boiler\_Site} \sum_{f\in BC} (C^{Boiler}_{Invest}{}_{ef} + \sum_{g\in T_{Boiler}} \tau_g.(C^{Boiler}_{Op}{}_{efg} + C^{Boiler}_{M}{}_{efg} + C^{Boiler}_{EM}{}_{efg})) \quad (4)$$

$$C^{Boiler}_{EM\ efg} = EM^{Boiler}_{CO_2}{}_{efg}.EMC_{CO_2}{}_{efg} + EM^{Boiler}_{SO_2}{}_{efg}.EMC_{SO_2}{}_{efg} + EM^{Boiler}_{NO_X}{}_{efg}.EMC_{NO_X}{}_{efg} \quad (5)$$

$$C_{ACH,CCH} = \begin{pmatrix} \sigma. \sum_{i\in ACH\_Site} \sum_{j\in ACHC} (C^{ACH}_{Invest}{}_{ij} + \sum_{k\in T_{ACH}} \tau_k.(C^{ACH}_{Op}{}_{ijk} + C^{ACH}_{M}{}_{ijk})) \\ \sigma. \sum_{i'\in CCH\_Site} \sum_{j'\in CCHC} (C^{CCH}_{Invest}{}_{i'j'} + \sum_{k'\in T_{CCH}} \tau_{k'}.(C^{CCH}_{Op}{}_{i'j'k'} + C^{CCH}_{M}{}_{i'j'k'})) \end{pmatrix} \quad (6)$$

$$C_{ESS,CSS} = \begin{pmatrix} \sigma. \sum_{a'\in ESS\_Site} \sum_{b'\in ESSC} (C^{ESS}_{Inv}{}_{a'b'}.Cap^{ESS} + \sum_{d'\in T_{ESS}} \tau_{d'}.(C^{ESS}_{Op}{}_{a'b'd'} + C^{ESS}_{M}{}_{a'b'd'})) \\ \sigma. \sum_{a"\in CSS\_Site} \sum_{b"\in CSSC} (C^{CSS}_{Inv}{}_{a"b"}.Cap^{CSS} + \sum_{d"\in T_{CSS}} \tau_k.(C^{CSS}_{Op}{}_{a"b"d"} + C^{CSS}_{M}{}_{a"b"d"})) \end{pmatrix} \quad (7)$$

EM and EMC are the pollutant emission and emission costs, respectively.

The installation costs of electric feeders, DHS, and DCS pipelines can be defined as a function of the capacity and the length of the routing path. Thus, the electric feeder cost (C_{Feeder}), DCS pipe cost (C_{Pipe_DCS}), and DHS pipe cost (C_{Pipe_DHS}) can be written as (8-10):

$$C_{Feeder} = \sigma \sum_{m\in Trans\cup CHP\_Site} \sum_{n\in Load\_Site} L_{mn}.\left((C^{Feeder}_{Capacity}\cdot Cap^{Feeder}_{mn} + C^{Feeder}_{leng})\right) \quad (8)$$

$$C_{Pipe\_DHS,Pipe\_DCS} = \sigma \sum_{m' \in DHC\_Site} \sum_{n' \in HCL\_Site} L_{m'n'} \begin{pmatrix} (C^{DH}_{Capacity} \cdot Cap_{m'n'} + C^{DH}_{leng}) \\ + (C^{DC}_{Capacity} \cdot Cap_{m'n'} + C^{DC}_{leng}) \end{pmatrix} \quad (9)$$

$$Cap = \rho_{water} . \pi \left(R^{DHC} \right)^2 . \zeta . \chi_{\max} \cdot \Delta\theta_{(input-output)} \quad (10)$$

The installation cost of the switching device is assumed a fixed parameter. The total interruption cost (C_{IC}) is the function of the electrical energy that is shed and the composite damage function of zonal electric load that is determined in the second stage problem [22].

$$C_{IC} = \sum_{\alpha=1}^{Ncont} \gamma_{\alpha} . P_{shed\ \alpha} . CDF_{\alpha} \quad (11)$$

The investment and maintenance costs of the PVA and SWT can be written as (12) and (13), respectively:

$$C_{PVA} = \sigma . \sum_{q \in PVA\_Site} (C^{PVA}_{Inv} \cdot A^{PVA}_{i} + C^{PVA}_{M}) \quad (12)$$

$$C_{SWT} = \sigma . \sum_{q' \in SWT\_Site} (C^{SWT}_{Invest} + C^{SWT}_{M}) \quad (13)$$

Electric power balance constraint of AMG can be written as (14):

$$\begin{aligned} P^{MG} = (& - \sum_{n \in Load\_site} P^{Load}_{n} + \sum_{q \in PVA\_Site} P^{PVA}_{q} + \sum_{a' \in ESS\_Site} P^{ESS}_{a'} + \\ & \sum_{q' \in SWT\_Site} P^{SWT}_{q'} + \sum_{a \in CHP\_Site} P^{CHP}_{a} - \sum_{i' \in ACH\_Site} P^{ACH}_{i'} \\ & - \sum_{i'' \in CCH\_Site} P^{CCH}_{i''} + \sum_{\beta \in DRPA} P^{DRP}_{\beta} - P^{Loss}) \end{aligned} \quad (14)$$

The energy purchased costs and energy sold benefits can be written as (15) and (16), respectively:

$$If\ P^{MG} > 0\ Then\ B_{Sell} = P^{MG} . \xi^{Elect}_{Sell}\ else\ C_{Purchase} = P^{MG} . \xi^{Elect}_{Purchased} \quad (15)$$

$$B_{DRP} = \Delta P^{TOU} . \xi^{Elect}_{Purchased} + \Delta P^{DLC} . \xi^{Elect}_{DLC} \quad (16)$$

The heating and cooling power balance constraint at the simulation interval can be written as (17) and (18), respectively [17]:

$$\begin{aligned} & - \sum_{n \in Load\_site} Q^{Load}_{n} + \sum_{e \in Boiler\_Site} Q^{B}_{e} - \sum_{i' \in ACH\_Site} Q^{ACH}_{i'} + \sum_{a \in CHP\_Site} Q^{CHP}_{a} - \\ & Q^{Loss} + \sum_{m' \in DHC\_Site} \sum_{n \in Load\_site} Q^{Flow}_{m'n} = 0 \end{aligned} \quad (17)$$

$$\begin{aligned} & - \sum_{n \in Load\_site} R^{Load}_{n} + \sum_{i'' \in CCH\_Site} R^{CCH}_{i''} + \sum_{i' \in ACH\_Site} R^{ACH}_{i'} - \\ & R^{Loss} + \sum_{a'' \in CSS\_Site} R^{CSS}_{i} + \sum_{m' \in DHC\_Site} \sum_{n \in CLoad\_site} R^{Flow}_{m'n} = 0 \end{aligned} \quad (18)$$

$$P^{CCH} = \frac{R^{CCH}}{COP_{CCH}} \tag{19}$$

$$Q^{ACH} = \frac{R^{ACH}}{COP_{ACH}} \tag{20}$$

$$\frac{R^{ACH}}{COP_{ACH}} \leq Q^{CHP} \tag{21}$$

A. CSS and ESS constraints:

The CSS is considered as a tank for chilled water storage and is modelled as [23]. The CSS constraints are maximum capacity, charge and discharge constraints, and mass balance constraints for each of the simulation interval.

CSS maximum capacity:

$$R^{CSS} \leq Cap^{CSS} \tag{22}$$

CSS maximum discharge and charge constraints:

$$RDC^{CSS} \leq (\vartheta \times Cap^{CSS}) \times X^{CSS} \qquad X^{CSS} \in \{0,1\} \tag{23}$$

$$RC^{CSS} \leq Cap^{CSS} \times Y^{CSS} \qquad Y^{CSS} \in \{0,1\} \tag{24}$$

CSS cannot discharge and charge at the same time:

$$X^{CSS}(t) + Y^{CSS}(t) \leq 1 \quad \forall\ t\ ,\ X^{CSS}\ and\ Y^{CSS} \in \{0,1\} \tag{25}$$

CSS maximum discharge and charge constraints are considered as [23].

The ESS constraints are maximum capacity, charge and discharge constraints, and power balance constraints for each of the simulation interval [24].

ESS maximum capacity:

$$P^{ESS} \leq Cap^{ESS} \tag{26}$$

ESS maximum discharge and charge constraints:

$$PDC^{ESS} \leq (\varpi . Cap^{ESS}) . X^{ESS} \qquad X^{ESS} \in \{0,1\} \tag{27}$$

$$PC^{ESS} \leq Cap^{ESS} . Y^{ESS} \qquad Y^{ESS} \in \{0,1\} \tag{28}$$

ESS maximum discharge and charge constraints are considered as [24].

ESS cannot discharge and charge at the same time:

$$X^{ESS}(t) + Y^{ESS}(t) \leq 1 \quad \forall\ t\ ,\ X^{ESS}\ and\ Y^{ESS} \in \{0,1\} \tag{29}$$

B. SWT and PVA constraints:

The SWT power generation equation can be written [25]:

$$P^{SWT} = \begin{cases} P_r^{Wind}.\dfrac{(v^{Wind} - v_c^{Wind})}{(v_r^{Wind} - v_c^{Wind})} & if\ v_c^{wind} \le v^{Wind} \le v_r^{wind} \\ P_r^{Wind} & if\ v_r^{wind} \le v^{Wind} \le v_f^{wind} \\ 0 & if\ v^{Wind} \le v_c^{Wind}\ or\ v^{Wind} \ge v_f^{Wind} \end{cases} \quad (30)$$

To ensure minimum noise disturbance in the AMG zones, the following constraint is considered [26]:

$$L_P \approx 50.\log_{10}.\Omega.R^{SWT} + 10.\log_{10}.R^{SWT} - 1 \quad (31)$$

The maximum power output of PVA can be written as [27]:

$$\mathrm{P^{PV}} = A^{PVA}.\eta.I.(1 - 0.005 \times (t_0 - 25)) \quad (32)$$

B. DHCN constraints:

The DHCN is modelled as [13] heating and cooling energy carriers are transferred to heating and cooling loads through separate lines. There are several DHCN constraints that consist of the entire heating and cooling load centres to be served constraints, flow direction constraints, DHCN device and pipe loading constraints.

The DHCN minimum and maximum flow constraints can be written as (33):

$$Q_{Min\ m'n}^{Flow} \le Q_{m'n}^{Flow} \le Q_{Max\ m'n}^{Flow} \quad \forall m' \in DHC\_Site, n \in Load\_site \quad (33)$$

C. CHP constraints:

Nonlinear feasible operating region for CHP units [28]:

$$\alpha'^{th}_{CHP} \times P^{CHP} + \beta'^{th}_{CHP} \times Q^{CHP} \ge \gamma'^{th}_{CHP} \quad (34)$$

$$P_{Min}^{CHP} \le P^{CHP} \le P_{Max}^{CHP} \quad (35)$$

$$Q_{Min}^{CHP} \le Q^{CHP} \le Q_{Max}^{CHP} \quad (36)$$

D. ACH and CCH constraints:

Feasible operating region for ACH and CCH units [15]:

$$R_{Min}^{X} \le R^{X} \le R_{Max}^{X} \quad \forall X \in CCH, ACH \quad (37)$$

$$Q_{Min}^{X} \le Q^{X} \le Q_{Max}^{X} \quad \forall X \in CCH, ACH \quad (38)$$

E. Boiler constraints:

Heat output limit for boilers:

$$Q_{Min}^{B} \le Q^{B} \le Q_{Max}^{B} \quad (39)$$

F. DRP constraints:

The AMG loads consist of critical, deferrable and controllable loads. Thus, the AMG can voluntary perform load shifting procedure for its deferrable loads based on TOU programs.

Further, the AMG can participate in the upward utility DLC program by reducing its controllable loads and change its power withdrawal from the utility grid. The upward utility can contract with the AMG to perform DLC procedure by paying a predefined fee. Hence, the DRP constraints for each bus of the system can be written as [28]:

$$P^{Load} = P^{Load}_{Critical} + P^{Load}_{Deferrable} + P^{Load}_{Controllable} \tag{40}$$

$$\Delta P^{TOU} = P^{Load}_{Deferrable} \tag{41}$$

$$\sum_{t=1}^{Period} \Delta P^{TOU} = 0 \tag{42}$$

$$\Delta P^{TOU}_{Min} \le \Delta P^{TOU} \le \Delta P^{TOU}_{Max} \tag{43}$$

$$\Delta P^{DLC}_{Min} \le \Delta P^{DLC} \le \Delta P^{DLC}_{Max} \ , \Delta P^{DLC}_{Max} = P^{Load}_{Controllable} \tag{44}$$

$$P^{DRP} = \Delta P^{DLC} + \Delta P^{TOU} \tag{45}$$

G. Electric network constraints:

The electric network constraints consist of electric feeders loading constraints, the load flow constraints, the entire electric load centres to be served constraints. The electric devices constraints can be represented as vector form:

$$\mathbf{P}^{Elec} = [\mathbf{P}^{Feeder}, \mathbf{P}^{PVA}, \mathbf{P}^{ESS}, \mathbf{P}^{SWT}, \mathbf{P}^{ESS}, \mathbf{P}^{ACH}, \mathbf{P}^{CCH}]^{Transpose} \tag{46}$$

$$\mathbf{P}^{Elec}_{Min} \le \mathbf{P}^{Elec} \le \mathbf{P}^{Elec}_{Max}$$

The integrated constraints of the first stage optimization problem can be represented as:

$$\Lambda_1(x,u,z) = 0 \tag{47}$$

$$\Gamma_1(x,u,z) \le 0 \tag{48}$$

Where, *x, u, z* are problem variables, controls and system topology, respectively.

2.2. Second Stage Problem Formulation

For the fixed first stage decision variables set of facilities installation, the second stage problem tries to find the optimal operational coordination of system resources in normal and contingent conditions. The optimal operational coordination of the AMG's resources in normal conditions can be represented as the operation cost minimization [22]:

$$Min\ \mathrm{S} = \sum_{j}^{Nzone} \begin{pmatrix} C^{CHP}_{Op\,j} + C^{Boiler}_{Op\,j} + C^{ACH}_{Op\,j} + C^{CCH}_{Op\,j} + C^{ESS}_{Op\,j} \\ + C^{CSS}_{Op\,j} + C_{Purchase} - B_{Sell} - B_{DRP} \end{pmatrix} \tag{49}$$

$$s.t.: \quad \Lambda_2(x,u,z) = 0$$
$$\Gamma_2(x,u,z) \le 0$$

Where $\Lambda_2(x,u,z) = 0$ and $\Gamma_2(x,u,z) \le 0$ are the detailed AC load flow model of the electric system of $\Lambda_1(x,u,z) = 0$ and $\Gamma_1(x,u,z) \le 0$, respectively.

The optimal operational coordination of the AMG's resources in contingent condition tries to minimize the current optimal dispatch costs of system resources plus the total interruption costs of the system. However, the control variables of the MG system under restoration conditions can be categorized as:

1. Discrete control variables of the system such as switching devices, and
2. Continuous control variables of the system resources.

The objective function of the second stage problem optimization at the contingent condition of the system can be represented as [22]:

$$Min\ \Xi = \sum_{j}^{Nzone} \left(\begin{array}{l} \Delta C_{Op\,j}^{CHP} + \Delta C_{Op\,j}^{Boiler} + \Delta C_{Op\,j}^{ACH} + \Delta C_{Op\,j}^{CCH} + \\ \Delta C_{Op\,j}^{ESS} + \Delta C_{Op\,j}^{CSS} + \sum_{\alpha=1}^{Ncont} \gamma_{\alpha} . P_{shed\ \alpha} . CDF_{\alpha} \end{array} \right) \tag{50}$$

$$s.t.: \quad \Lambda_2^{'\alpha}(x,u,z) = 0 \qquad \forall \alpha \in \{0,1,....,Ncont\}$$

$$\Gamma_2^{'\alpha}(x,u,z) \le 0$$

CDF is the customer damage function that determines the relationship between the economic loss of interruption (interruption cost) and the interruption duration.

Where $\Lambda_2^{'\alpha}(x,u,z) = 0$ and $\Gamma_2^{'\alpha}(x,u,z) \le 0$ are the detailed AC Security Constrained Optimal Power Flow (SCOPF) model of $\Lambda_1(x,u,z) = 0$ and $\Gamma_1(x,u,z) \le 0$, respectively.

3. Solution Algorithm

The proposed DERNEP has many binary and real decision variables and it can be formulated as a MINLP problem that consists of non-convex and nonlinear parameters. Fig. 2 depicts the schematic diagram of the DERNEP model.

The proposed model of DERNEP is a MINLP problem and has a large state space that involves thousands of variables in the expansion-planning horizon. The DERNEP objective function and constraints are nonlinear and non-convex. An iterative bi-level optimization algorithm is presented for solving the DERNEP problem. Fig. 3 depicts the flowchart of the optimization algorithm. The flowchart blocks are presented in the following paragraphs.

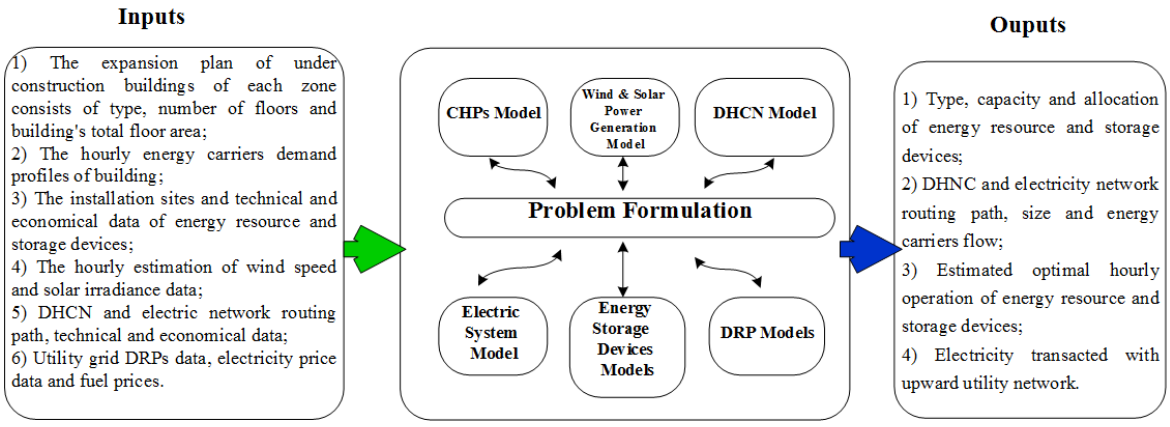

Fig. 2: Schematic diagram of the DERNEP model.

3.1. First stage optimization problem

The first stage optimization problem assumptions are:

1. The installed cooling, heating and electric facilities are working at their maximum capacity and their different capacity installation alternatives are estimated as a continuous variable.
2. The Direct Current (DC) load flow is used. The power factor of the system is assumed to be 1.0.
3. A monthly cooling, heating and electric loads are extracted from their corresponding hourly loads. The first stage optimization problem uses the monthly load curves.
4. The electric loss is estimated as a percent of the total system electric load. Further, heating and cooling loss are considered as a percent of total system heating and cooling loads, respectively. The energy loss will be modified in the second stage optimization problem.

For the first level optimization problem, a GA with variable fitness functions is used. The rates of the operators are adapted in a deterministic, reinforcement-based manner [22]. The behavior of each operator (that is, the specific way it operates) is modified by changing its parameter values. The first stage problem is optimized for the monthly period of the planning years.

To improve the performance and speed of the specified GA, a list of suitable candidates is selected for the first generation of the chromosomes. For the implementation of operational constraints in the optimization process, a penalty factor representation is used [22].

For the first stage problem, each chromosome can be an alternative to the allocation problem. For, example, the first stage problem has two set of decision variables for facility allocation:

a) The optimal capacity installation alternative,
b) The installation site.

Thus, each chromosome consists of two-part that the first part presents the installed capacity data; meanwhile, the second part presents the installation site data. The installed capacity variable and installation site variable are assumed as a continuous and discrete variable, respectively.

If the installation capacity alternative range is considered as [50kW 500 kW], the data of (51) will be decoded as follows:

$$\textit{First stage problem chromosome} = \left[1001101100110111011001110110011 0\right] \tag{51}$$

a) Decoding of capacity installation alternative for the first bus:

$$1\times 2^{14}+0\times 2^{13}+0\times 2^{12}+1\times 2^{11}+1\times 2^{10}+0\times 2^{9}+1\times 2^{8}+1\times 2^{7}+0\times 2^{6}$$
$$+0\times 2^{5}+1\times 2^{4}+1\times 2^{3}+0\times 2^{2}+1\times 2^{1}+1\times 2^{0}=\ 19867$$

$$\frac{19867}{2^{15}-1} = 0.6063 \Rightarrow P_{CHP\_1} = 0.6063 \times (500-50) + 50 = 322.8\ \text{kW}$$

b) Decoding of capacity installation alternative for the first bus:

$$1\times 2^{14} + 0\times 2^{13} + 1\times 2^{12} + 1\times 2^{11} + 0\times 2^{10} + 0\times 2^{9} + 1\times 2^{8} + 1\times 2^{7} + 1\times 2^{6} + 0\times 2^{5} + 1\times 2^{4} + 1\times 2^{3} + 0\times 2^{2} + 0\times 2^{1} + 1\times 2^{0} = 23001$$

$$\frac{23001}{2^{15}-1} = 0.7020 \Rightarrow P_{CHP\_2} = 0.7020(500-50) + 50 = 365.9\ \text{kW}$$

Thus, the installation capacity alternatives for the first and second bus are 322.8 kW and 365.9 kW, respectively.

The second part of the chromosome proposes to install the 322.8 kW facility on the first bus.

The final optimization fitness function of the first stage problem can be written as [22]:

$$\text{Max } \mathbf{Z}' = \boldsymbol{M}' - \mathbf{Z} - \boldsymbol{W}.\Lambda(\boldsymbol{u},\boldsymbol{x},\boldsymbol{z}) - \boldsymbol{W}'.\Gamma(\boldsymbol{u},\boldsymbol{x},\boldsymbol{z}) \quad (52)$$

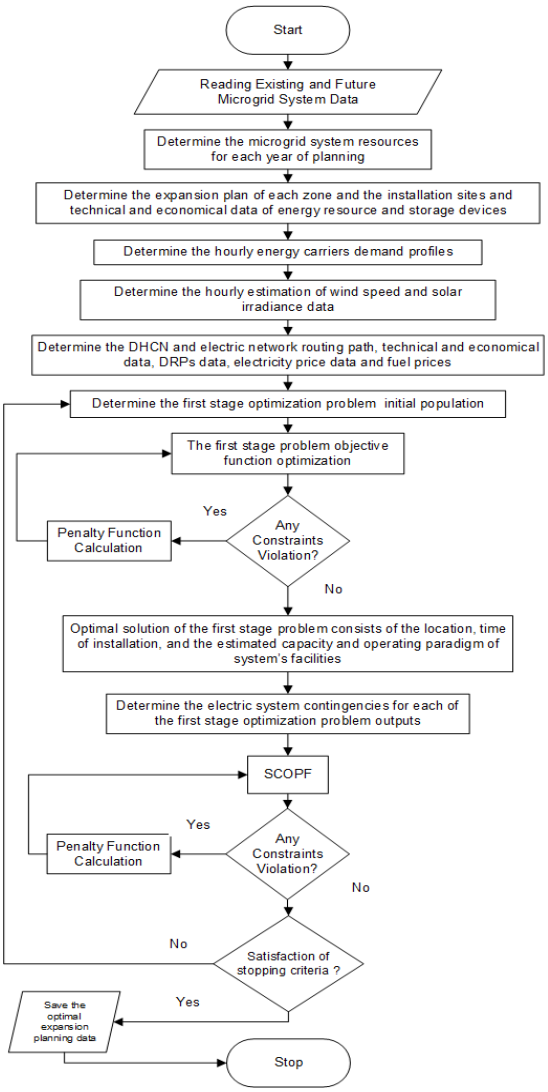

Fig. 3: Flowchart of the DERNEP algorithm.

Where, $\mathbf{Z}'$ and *M'* are objective function and high number vectors, respectively. *W* and *W'* are weight factor vectors that can be increased linearly through iterations from zero to a very high number.

3.2. Second stage optimization problem

At the first stage, the location, time of installation, and the estimated capacity and operating paradigm of system's facilities are determined and the capacity installation alternatives of cooling, heating and electric facilities are assumed as a continuous variable. However, at the second stage, the capacity installation alternatives of facilities are changed to their corresponding available capacity based on their maximum and minimum energy generation constraints. For example, if the first stage optimization algorithm proposes a 4115 kW CHP system and the available set of CHP systems are as:

Available capacity of CHP system set = {1210 kW, 4600 kW}.

The second stage will consider the following installation alternatives as:

The second stage installation alternative set = {4×1210 kW, 4600 kW}.

The SCOPF of the second stage optimization problem explores the detailed optimal operation of cooling, heating and electric systems based on their corresponding hourly load curves. It investigates the adequacy of system resources for the most important loads based on the 'N-1' concept. For a fixed location of switching devices that are their locations are determined at the first stage problem, the second stage problem uses the switching ability and optimal resource operational coordination under contingent conditions [22]. After an electrical system contingency, it is assumed that 'N-1' resource components of the electric system are available and may be sufficient to ensure full functioning. The SCOPF problem simulates the outage of one component of the electric system and it tries to find the optimal coordination of other system resources after the switching of switching devices. If the electrical system resources are not adequate to supply electricity of the MG and the upward utility electricity is not available, then the SCOPF considers the Load Shedding Procedure (LSP). The LSP uses the following algorithm:

1- At first, the MG's controllable loads $(P_{Controllable}^{Load})$ are turned off,

2- If the electric power balance constraint of MG is not satisfied, then turn off the deferrable load blocks $(P_{Deferrable}^{Load})$,

3- P_{shed} is the total shed load.

Electric system loss of (1) is calculated from the detailed AC load flow.

The optimization fitness function of the second stage problem can be written as [22]:

$$\text{Max } \Xi^{'} = \boldsymbol{M}''-\Xi-\boldsymbol{W}''.\Lambda_2^{'\boldsymbol{\alpha}}(\boldsymbol{u},\boldsymbol{x},\boldsymbol{z})-\boldsymbol{W}'''.\Gamma_2^{'\boldsymbol{\alpha}}(\boldsymbol{u},\boldsymbol{x},\boldsymbol{z}) \tag{53}$$

Where, $\Xi^{'}$ and *M''* are objective function and high number vectors, respectively. *W''* and *W'''* are weight factor vectors that can be increased linearly through iterations from zero to a very high number.

The Weighted Reliability Index (WRI) is used for stopping criteria, defined as:

$$WRI = wf^{'}_{1} * SAIDI + wf^{'}_{2} * SAIFI \tag{54}$$

Where,

$SAIFI$= Total number of system interruptions/ total number of building blocks served. (55)

$SAIDI$ = Sum of the interruption duration / total number of buildings blocks. (56)

$wf^{'}_{1}$, $wf^{'}_{2}$ are weight factor vectors.

4. Simulation Results

The proposed algorithm was applied to a building complex. The building complex consists of five zones and 42 buildings and its total area is about 56 hectare. At the horizon year, the number of buildings will increase to 67 buildings. The expansion planning consists of the construction of new buildings. The time horizon is chosen the year 2023, or 5 years into the future and the DERNEP is performed for 5 years planning horizon. Fig. 4 show the expansion planning of the building complex.

Data-loggers were installed to extract the existing buildings electrical load profiles and annual heating, cooling and electrical loads of under construction buildings were estimated by an energy simulation software. Monthly cooling, heating and electric loads are extracted from their corresponding hourly loads for expansion planning horizon. The monthly energy carrier load can be written as a function of its hourly load as:

$$Monthly\ \ Load = \frac{\int_0^{T_1} Hourly\ \ Load}{T_1} \tag{57}$$

Where, T_1 is the total monthly hours.

Fig. 5 shows the estimated zones heating, cooling and electrical load profiles at the horizon year. CHPs were selected based on the best available technology [29]. Tables 2 and Fig. 6 show the characteristics of CHPs and boilers, respectively. The maintenance cost and lifetime of boilers are 4.81E+05 (MUs) and 25 years, respectively.

Fig. 4. Expansion planning map of the building complex.

Table 2. CHP data [29].

	Taurus60	Centaure50	Centaure40	Saturn20
Output power (kW)	5200	4600	3515	1210
Electrical efficiency (%)	30.3	29.3	27.9	24.4
Investment cost (MUs/MW)	3.01E+10	3.09E+10	3.27E+10	4.11E+10
Lifetime	20			
Maintenance cost	C_{M}^{CHP} =7.4E+05(MUs/MWh)			

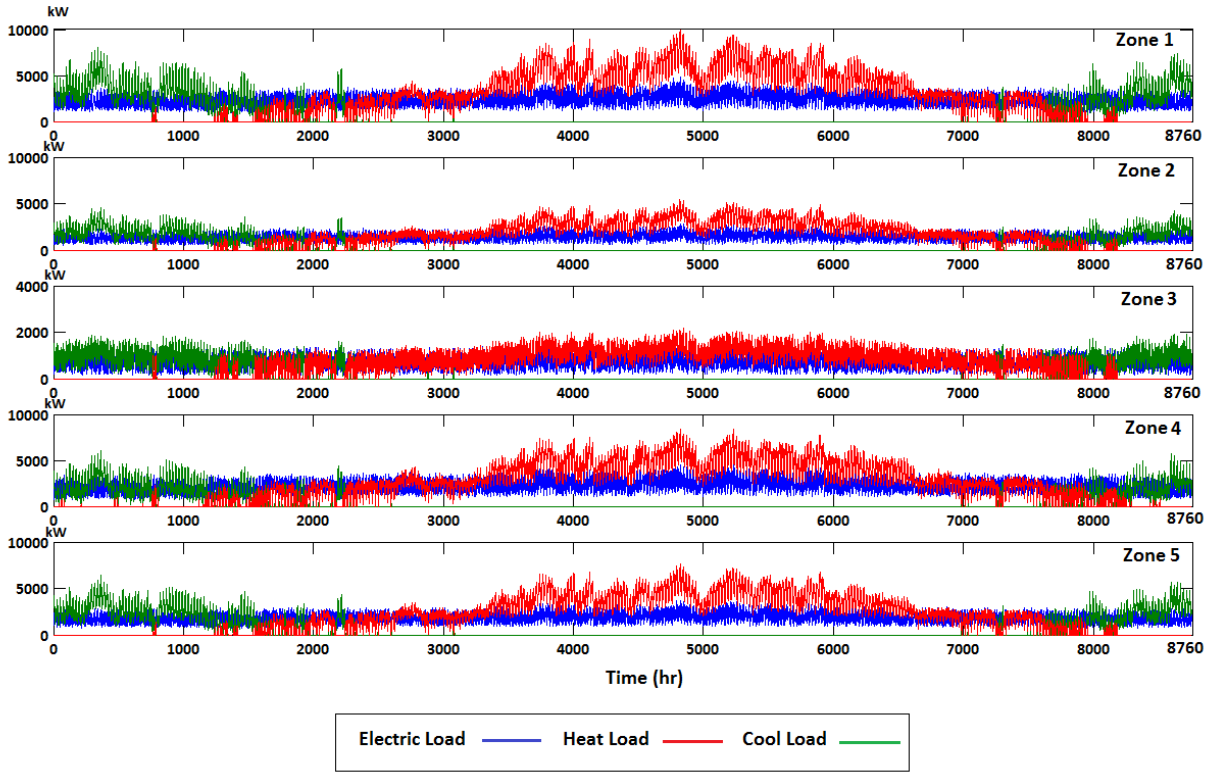

Fig. 5. Zones heating, cooling and electrical load profiles at the horizon year.

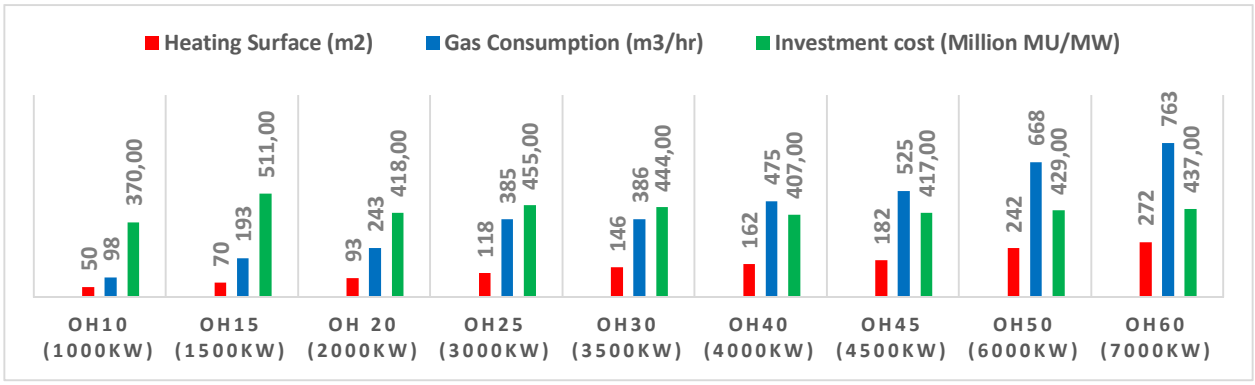

Fig. 6 Boilers data [30].

Table 3. shows the DERs, DHCN and electric feeder data. Table 4, presents gas price and the environmental emission costs.

Table 3. DERs, DHCN and electric feeder data [31-34].

	parameters
PVA	C_{Inv}^{PVA} = 1.48E+5 (MMUs/ MW), Lifetime=25(years), C_{M}^{PVA} =5.55E+01 (MMUs/MWh)
SWT	3.5(kW) @ 250 (rpm), Cut-in speed= 3(m/s), Total length=3 (m), Type: Up-wind horizontal rotor, noise: 37 dB(A) from 60 (m) with a wind speed 8 (m/s) , C_{Invest}^{SWT} =2.4E+03 (MMUs), C_{M}^{SWT} =3.7E+04 (MUs/MWh)
ACH	C_{Invest}^{ACH} =4.0811E+03 (MMUs), C_{Op}^{ACH} =6.4195E+03 (MMUs/MWh), C_{M}^{ACH} =3.81E+04 (MUs/MWh), COP=0.81, Lifetime=25(years)
CCH	C_{Invest}^{CCH} =4.218E+03 (MMUs), C_{Op}^{CCH} =4.736E+03 (MMUs/MWh), C_{M}^{CCH} =3.77E+04 (MUs/MWh), COP=4, Lifetime=25(years)
ESS	Max capacity=10 (MW), Modules capacity= 100 (kW), Type: Lead-acid battery, Efficiency=0.75, C_{Inv}^{ESS} =11.285E+03 (MMUs/MWh), $C_{Op}^{ESS} + C_{M}^{ESS}$ =5.55E+02 (MMUs/MWh), Lifetime=3500 (cycle number)
CSS	C_{Inv}^{CSS} = 5.55E+02 (MMUs/MWh) , $C_{Op}^{ESS} + C_{M}^{ESS}$ =1.2E+01 (MMUs/MWh), Lifetime=25(years)
DHCN	$C_{Capacity}^{DH}$ =2.59 (MMUs/m.MW), C_{leng}^{DH} =1.221E+01 (MMUs/m), $C_{Capacity}^{DC}$ =2.59 (MMUs/m.MW), C_{leng}^{DC} =1.221E+01 (MMUs/m), Q^{Loss} =%18 heating transmission, R^{Loss} = %7 cooling transmission
Feeder	$C_{Capacity}^{Feeder}$ =143267 (MUs/kW), C_{leng}^{Feeder} = 32641 (MUs/m)
Environmental emission prices	C_{CO_2} =2.59 (MMUs/ton), C_{SO_2} =3.7E+01 (MMUs/ton), C_{NO_X} =3.7E+01 (MMUs/ton),

Table 4. Gas prices, interruption and environmental emission costs [35].

Parameter	Price	Parameter	Price
Natural gas fuel (MMUs/m^3)	0.03	NO_X emission cost (MMUs/kg)	0.37
SO_2 emission cost (MMUs/kg)	0.37	CO_2 emission cost (MMUs/ton)	2.59
Interruption cost of zone 1,2,4,5 (MMUs/kWh)	0.42	Interruption cost of zone 3 (MMUs/kWh)	0.38

The mean 30-year hourly average solar radiation, wind speed, and ambient temperature of the building complex site are available at [36, 37], respectively.

Different scenarios were studied in the following cases to assess the proposed DERNEP algorithm:

Scenario 1: The microgrid purchased electricity from the utility grid to supply its loads. Only boilers and CCHs were used to supply heating and cooling loads, respectively.

Scenario 2: The microgrid installed CCHP systems. The heating and cooling loads of zones could be connected to other zones' CCHPs through DHCN. Further, the surplus electricity of zones could be sold to the upward utility grid.

Scenario 3: The microgrid implemented the 2nd scenario alternatives and it installed SWTs, PVAs and ESSs.

Scenario 4: The AMG implemented the 3rd scenario alternatives and it installed CSSs and participated in the utility's TOU programs.

Scenario 5: The AMG implemented the 4th scenario alternatives and it participated in the upward utility DLC programs. First, the upward utility proposed the fee option of DLC procedure. Then, the DERNEP determined the optimum value of DLC for different zones that led to maximum AMG's benefit.

As shown in Fig. 7, the electricity sold price of the 2nd and 3rd scenarios is about 250 percent of the electricity purchased price based on the fact that the upward utility company encourages the energy infrastructure investments. Further, the electricity sold price of the 4th and 5th scenarios is about 125 percent of TOU based electricity purchased price. Fig. 8 presents the TOU and DLC parameters for the 4th and 5th scenarios.

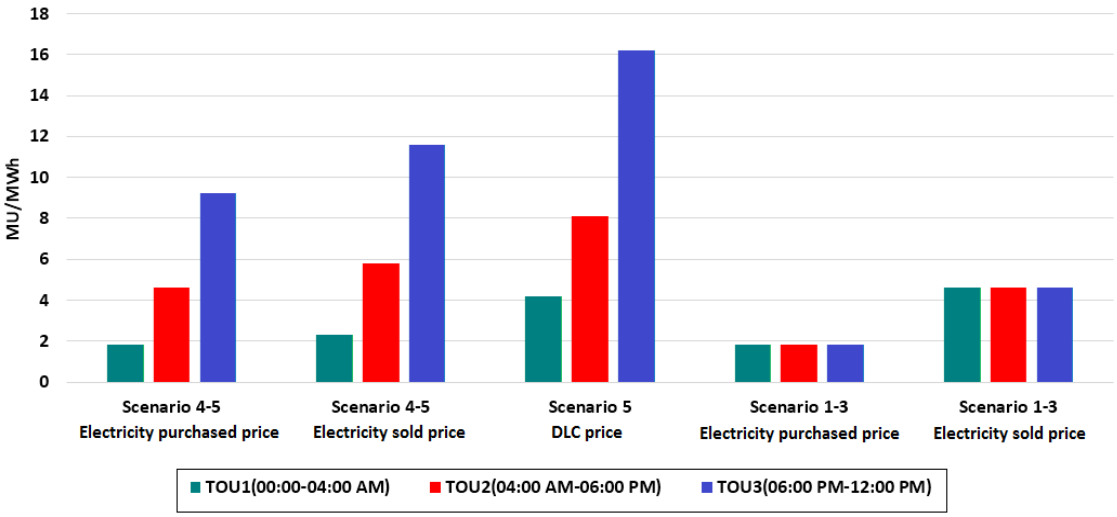

Fig. 7. The electricity price for different scenarios.

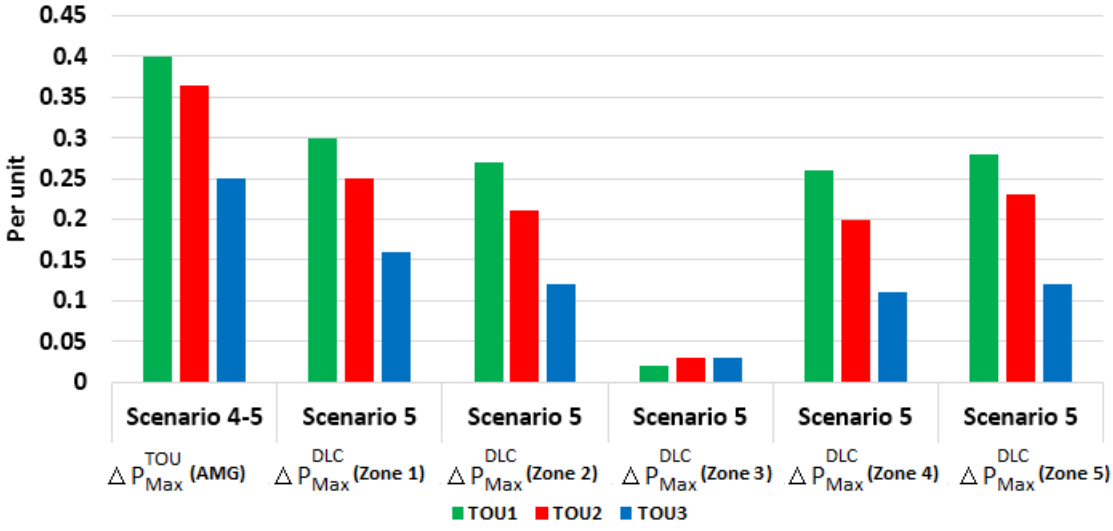

Fig. 8. The DLC parameters for the 4th and 5th scenarios.

The stochastic single order independent failures are considered as contingencies. The reliability data which is used can be categorized as:

- Single independent device failure of the internal system of MG, in which their failure rates are extracted from the database,
- The faults of the cables of the MG to the upward utility.

For each contingency scenario, the problem optimizes cost allocation. The stopping criterion was selected as $WRI < 2.5$ with $wf'_1 = wf'_2 = 0.5$ or the number of iterations > 3000.

The proposed method was solved for expansion planning horizon. The algorithm codes were developed in MATLAB and the simulation was carried out on a PC (Intel Core 2, 2.93 GHz, 4 GB RAM). Table 5 shows the number of continuous and discrete variables and the number of equations for 1-5 scenarios. The Number of Optimization Equations (NOE) consists of main equality equations and converted inequality equations to equality equations by adding slack variables. The NOE for the 5th scenario is 4956450 that indicates the curse of dimensionality and the maximum CPU time required to solve the scenarios was about 3621 seconds.

Table 5: Number of variables of the system for different scenarios.

Case	Continuous variables	Discrete variables	NOE
Scenario 1	653549	13133	1244223
Scenario 2	1973080	63600	3197410
Scenario 3	2803488	27846	4580294
Scenario 4	2804202	38804	4567332
Scenario 5	3113560	63600	4956450

Table 6 displays the AMG's optimal allocation, capacity and equipment characteristics for different scenarios. As shown in table 6, no DERs were installed for the 1st scenario and the heating and cooling loads were supplied by boilers and compression chillers, respectively. At the first year of expansion planning of 2nd scenario, the DERNEP installed two 1210 kW CHPs in the zone 2 and the surplus of heating and cooling energy generations were transferred to the zone 1 and zone 5; meanwhile, the surplus electricity of the zone 2 was sold to the upward utility grid. At the final year of expansion of the 2nd scenario, more 1210 kW CHPs were installed in the AMG' zones and more surplus electricity were sold to the upward utility.

The DERNEP installed the maximum PVA capacity at the 5th year of expansion planning of the 3rd scenario and the installed capacity of boilers and absorption chillers were highly reduced with respect to the 2nd scenario; meanwhile, the installed capacity of compression chillers was highly increased. The installed capacity of CHP was remained constant for the 4th and 5th scenarios, while the DERNEP installed more CSS and ESS for the 5th scenario with respect to 4th scenario based on the fact that CSS and ESS improve the rapid response ability of MG to handle the utility's DRP programs.

Table 6. Final DERNEP results.

Scenario	1	1	2	2	3	3	4	4	5	5
Year of Expansion planning	1	5	1	5	1	5	1	5	1	5
CHPs (kW)										
Zone 1	0	0	1210	3×1210	1210	1210	1210	1210	1210	1210
Zone 2	0	0	2×1210	3×1210	2×1210	3×1210	2×1210	3×1210	2×1210	3×1210
Zone 3	0	0	0	0	0	0	0	0	0	0
Zone 4	0	0	1210	3×1210	1210	2×1210	1210	2×1210	1210	2×1210
Zone 5	0	0	1210	1210	1210	1210	1210	1210	1210	1210
Boilers (kW)										
Zone 1	4000	2×4000	0	0	0	2×2000	0	2×2000	0	2×2000
Zone 2	3000	2×3000	3000	3000	3000	3000	3000	3000	3000	3000
Zone 3	1000	2×1000	1000	2×1000	1000	2×1000	1000	2×1000	1000	2×1000
Zone 4	3500	2×3500	1000	1000	1000	2×1000	1000	2×1000	1000	2×1000
Zone 5	3000	2×3000	0	2500	0	2500	0	2500	0	2500
ACH (kW)										
Zone 1	0	0	1700	3×1700	1700	1700	1700	1700	1700	1700
Zone 2	0	0	1700	2×1700	1700	2×1700	1700	2×1700	1700	2×1700
Zone 3	0	0	0	0	0	0	0	0	0	0
Zone 4	0	0	1700	3×1700	1700	2×1700	1700	2×1700	1700	2×1700
Zone 5	0	0	1700	1700	1700	1700	1700	1700	1700	1700
CCH (kW)										
Zone 1	5500	2×5500	3000	2×3000	3000	2×3000	3000	2×3000	3000	2×3000
Zone 2	3000	2×3000	0	1000	0	1000	0	1000	0	1000
Zone 3	2000	2000	2000	2000	2000	2000	2000	2000	2000	2000
Zone 4	4500	2×4500	2500	2500	2500	2×2500	2500	2×2500	2500	2×2500
Zone 5	4500	2×4500	3000	2×3000	3000	2×3000	3000	2×3000	3000	2×3000
PVA (kW)										
Zone 1	0	0	0	0	3000	4500	3000	4500	3000	4500
Zone 2	0	0	0	0	4000	4000	4000	4000	4000	4000
Zone 3	0	0	0	0	4000	4000	4000	4000	4000	4000
Zone 4	0	0	0	0	4000	4000	4000	4000	4000	4000
Zone 5	0	0	0	0	2000	4000	2000	4000	2000	4000
SWT (kW)										
Zone 2	0	0	0	0	8×3.5	8×3.5	8×3.5	8×3.5	8×3.5	8×3.5
Zone 3	0	0	0	0	16×3.5	16×3.5	16×3.5	16×3.5	16×3.5	16×3.5
ESS (kWh)										
Zone 2	0	0	0	0	5×100	5×100	5×100	5×100	5×100	5×100
Zone 3	0	0	0	0	10×100	10×100	10×100	10×100	10×100	10×100
CSS (MWh)										
Zone 1	0	0	0	0	0	0	0	4.64	0	4.64
Zone 2	0	0	0	0	0	0	0	0	12.75	12.75
Zone 3	0	0	0	0	0	0	0	0	0	0
Zone 4	0	0	0	0	0	0	0	6.95	0	6.95
Zone 5	0	0	0	0	0	0	0	12.75	0	12.75
District heating and cooling pipe (kWh)	--	--	Zone 2 to Zone 1 (1900) and Zone 5 (1900)	Zone 2 to Zone 1 (1900) and Zone 5 (1900)	Zone 2 to Zone 1 (1900) and Zone 5 (1900)	Zone 2 to Zone 1 (1900) and Zone 5 (1900)	Zone 2 to Zone 1 (1900) and Zone 5 (1900)	Zone 2 to Zone 1 (1900) and Zone 5 (1900)	Zone 2 to Zone 1 (1900) and Zone 5 (1900)	Zone 2 to Zone 1 (1900) and Zone 5 (1900)

The DERNEP proposed that the heating loads of zone 1 and zone 5 were connected to the zone 2 heating source through a district heating network.

The final electric network of AMG at the horizon year of 5th scenario is shown in Fig. 9. The PVAs were roof-mounted panels that were installed on the roof of the buildings.

The final optimum topology of the microgrid had 219 independent failures for the 5th scenario.

In the following paragraphs, the analysis of the second stage optimization problem is presented and the optimal facilities dispatch scheduling is shown in hourly dispatch diagram. Fig.10 (a) and (b) depict the stacked column of the estimated values of the optimal heating and electricity dispatch for the 2nd scenario of the 1st zone and third week of January 2023, respectively.

The CHPs were committed based on the DERNEP optimal dispatch outputs and the DH network transferred heat from the second zone to the first zone. The first zone imported heat from the second zone and the produced heat by the CHPs did not satisfy all heat requirements of the first zone.

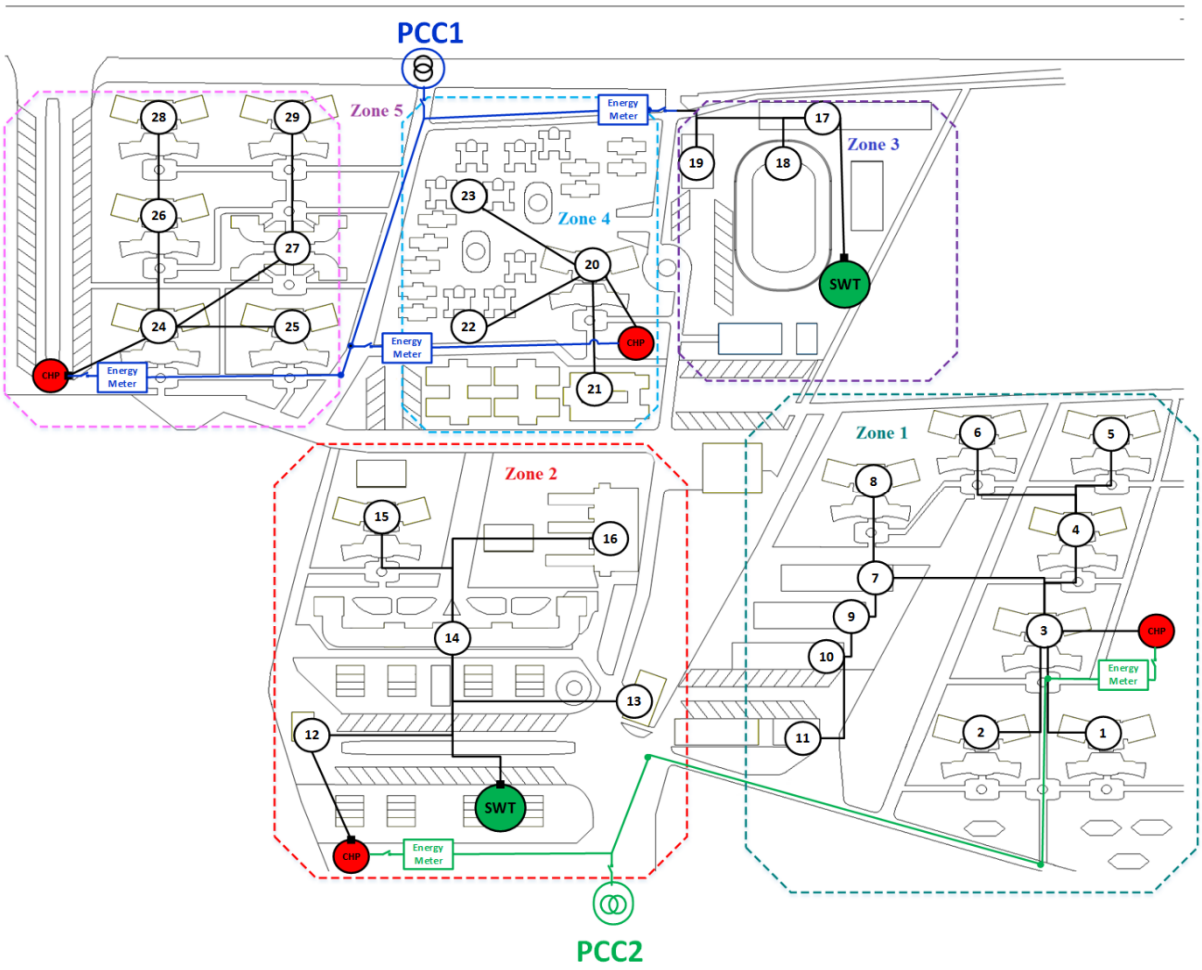

Fig. 9. The final electric network of AMG at the horizon year of planning for the 5th scenario.

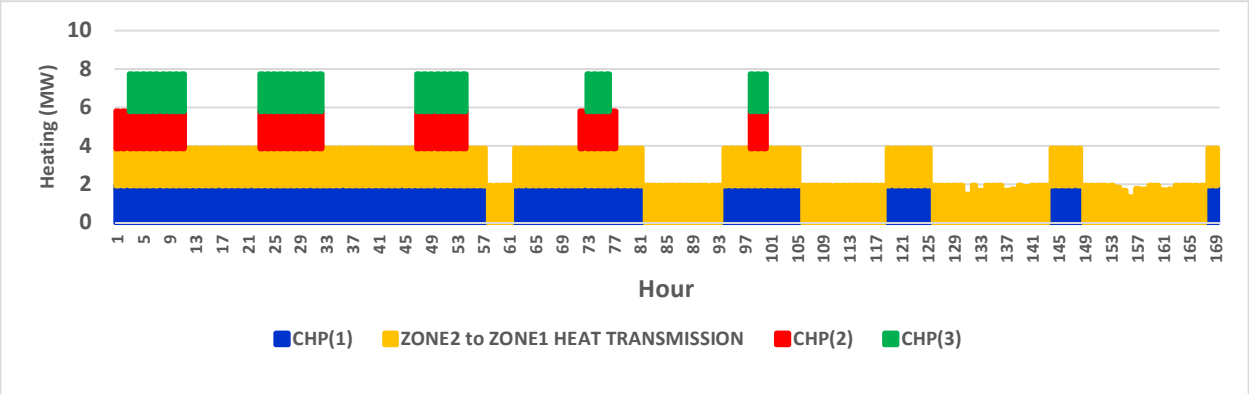

(a)

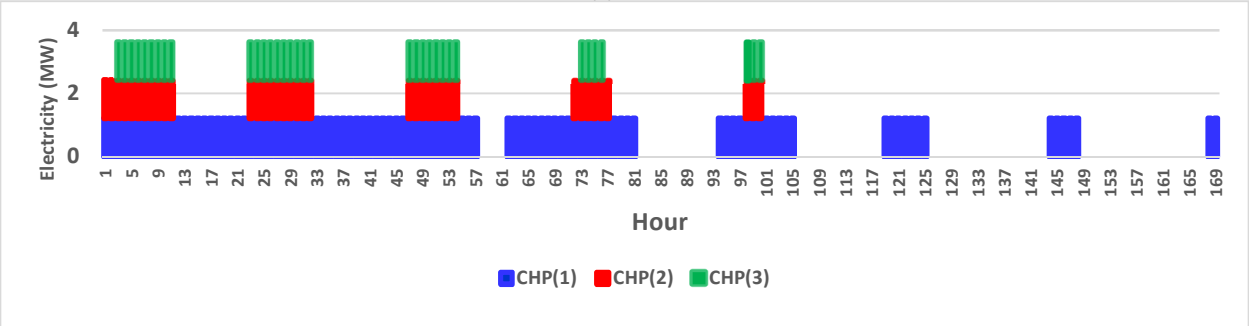

(b)

Fig.10. (a) The stacked column of the estimated optimal heating dispatch for the 2nd scenario of the 1st zone and third week of January 2023. (b) The stacked column of the estimated optimal electricity dispatch for the 2nd scenario of the 1st zone and third week of January 2023.

Fig. 11 shows the stacked column of the estimated optimal cooling dispatch of the 1st zone for the 2nd scenario and the first week of September 2023. The absorption chillers were at full load and the electrical chillers were following the cooling load. The second electrical chiller was partially loaded when the cooling load of the zone was higher.

Fig.12 (a) and (b) depict the stacked column of the estimated optimal heating and electricity dispatch for the 3rd scenario of the 4th zone and second week of June 2023, respectively. The CHPs were at full load when they committed and the boiler tracked the heating load.

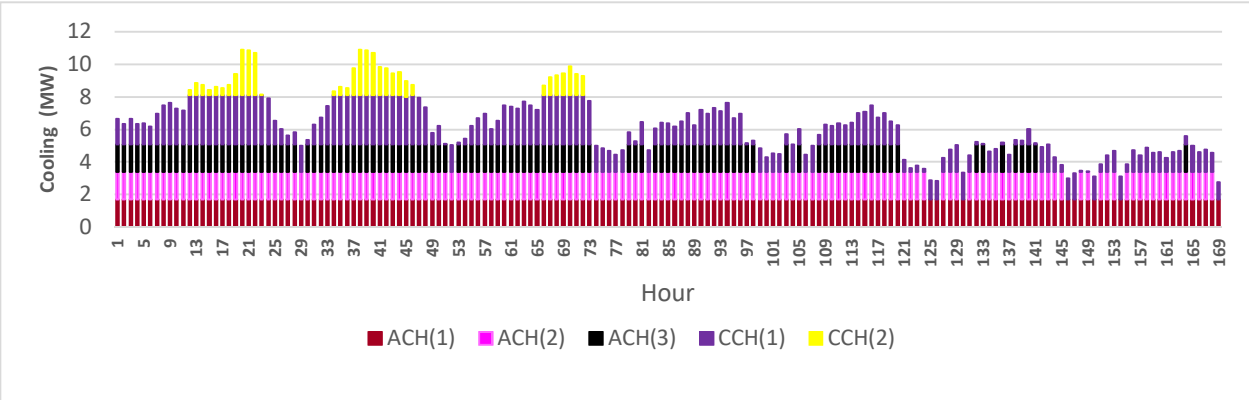

Fig. 11. The stacked column of the estimated optimal cooling dispatch of the 1st zone for the 2nd scenario and the first week of September 2023.

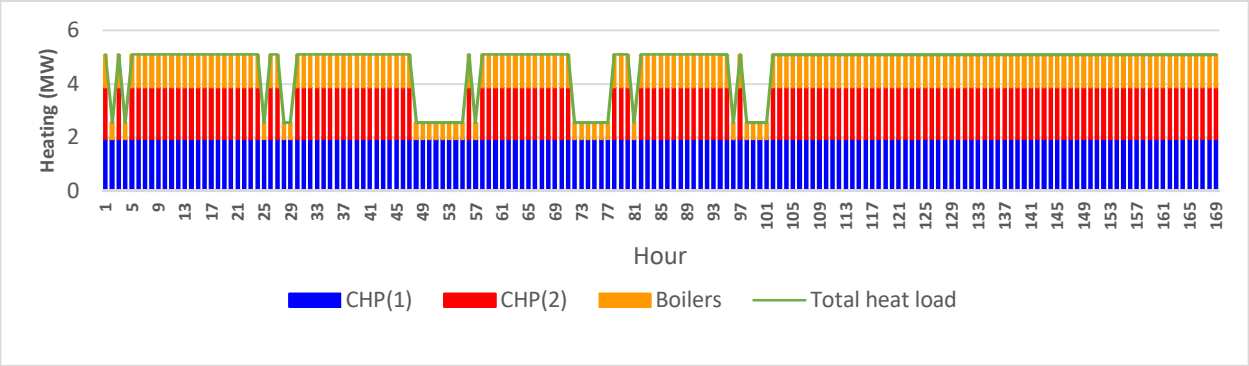

(a)

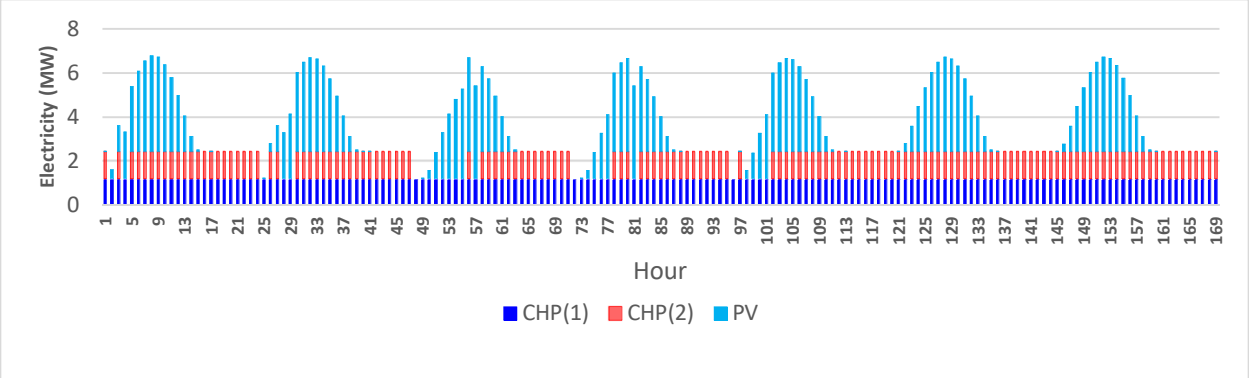

(b)

Fig.12 (a) The stacked column of the estimated optimal heating dispatch for the 3rd scenario of the 4th zone and second week of June 2023. (b) The stacked column of optimal electricity dispatch for the 3rd scenario of the 4th zone and second week of June 2023.

Fig. 13 shows the stacked column of the estimated optimal cooling dispatch of the 1st zone for the 3rd scenario and the second week of August 2023. The absorption chillers were fully loaded when they were on. The first and second electrical chillers of the 1st zone were partially loaded and the CCH (2) was committed when the cooling load of the zone reached its maximum value.

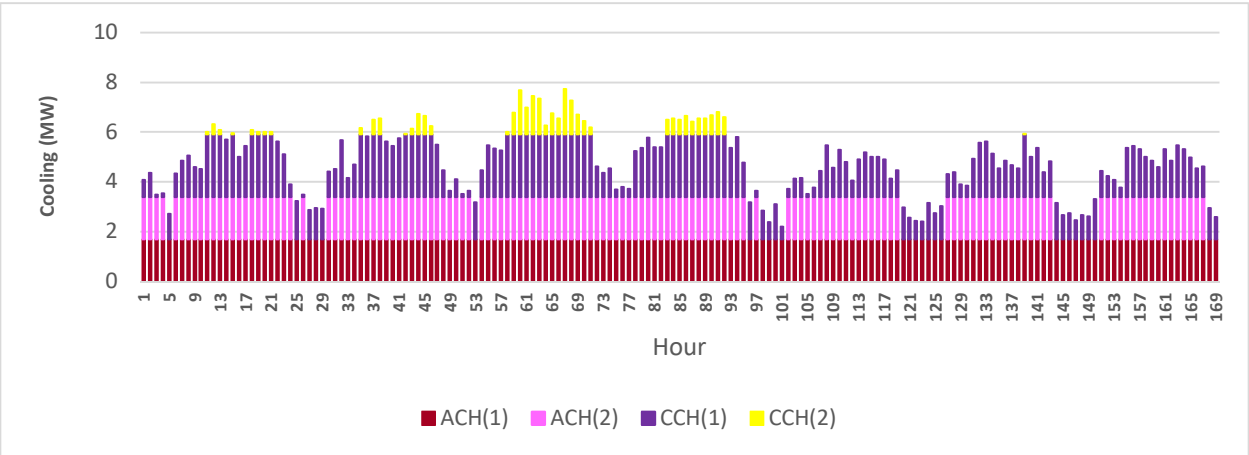

Fig. 13. The stacked column of the estimated optimal cooling dispatch of the 1st zone for the 3rd scenario and the second week of August 2023.

Fig.14 (a) and (b) show the estimated values of the 5th zone optimal heating and electricity dispatch for the 4th scenario and the second week of January 2023, respectively.
The boilers of the 5th zone were always at partial load when they were on; on the other hand, its CHP was at full load when it was on.

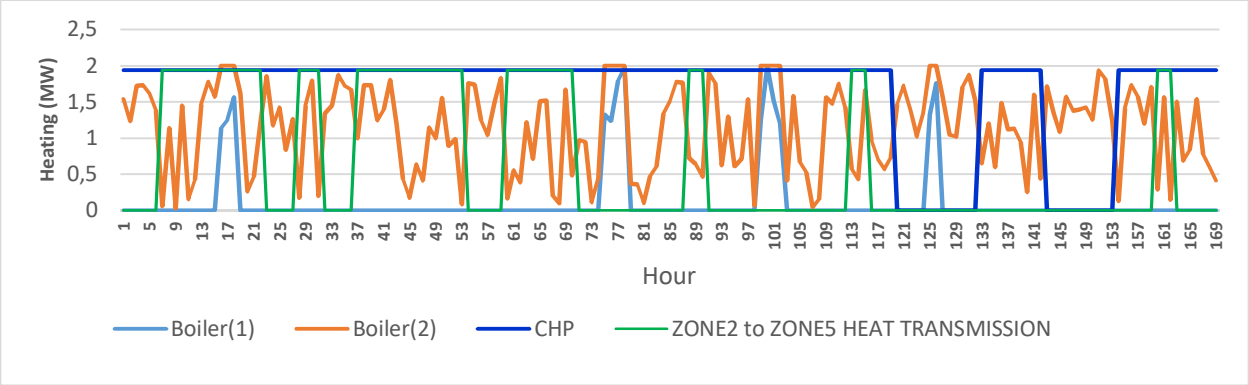

(a)

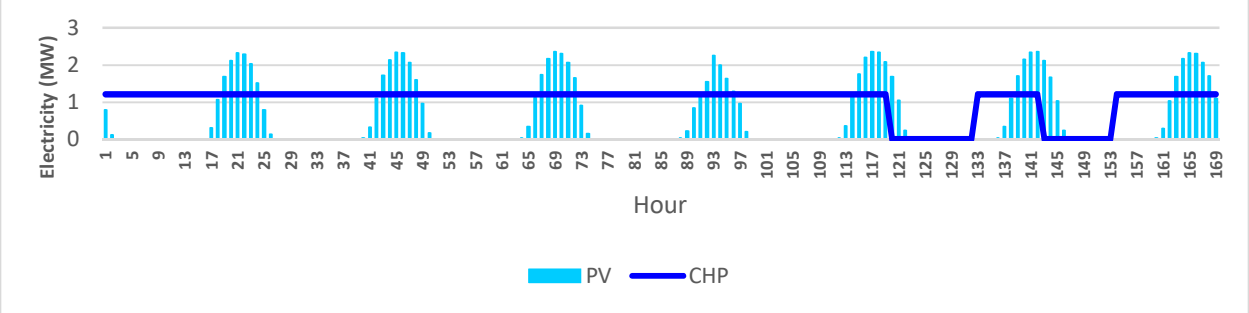

(b)

Fig.14. (a) The estimated values of 5th zone optimal heating dispatch for the 4th scenario and second week of January 2023. (b) The estimated values of 5th zone optimal electricity dispatch for the 4th scenario and second week of January 2023.

Fig. 15 (a), (b) show the stacked column of the estimated values of the 5th zone optimal cooling dispatch and the estimated values of cooling storage charge and discharge for the 4th scenario and the second week of July 2023, respectively. The ACH (1) and CCH (1) were fully committed and the CCH (2) was committed when the cooling load of the zone reached its maximum value.
Fig.16 (a) and (b) show the stacked column of the estimated values of the 5th zone optimal heating and electricity dispatch for the 5th scenario and the second week of June 2023, respectively. The CHPs were fully committed and the boiler tracked the heating load.
Fig. 17 (a) and (b) show the stacked column of the estimated values of the 5th zone optimal cooling dispatch and cooling storage charge and discharge for the 5th scenario and the first week of June 2023, respectively. The absorption chiller was at full load and the electrical chillers tracked the cooling load.

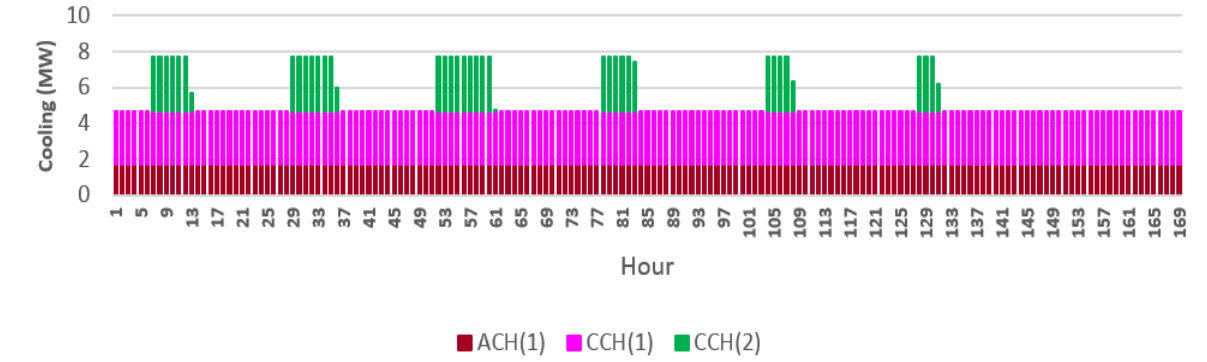

(a)

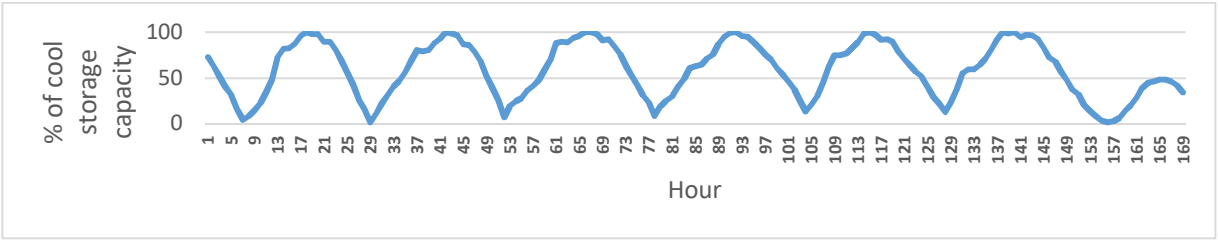

(b)

Fig. 15. (a) The stacked column of the estimated values of 5th zone optimal cooling dispatch for the 4th scenario and the second week of July 2023. (b) The estimated values of 5th zone optimal cooling storage charge and discharge for the 4th scenario and the second week of July 2023.

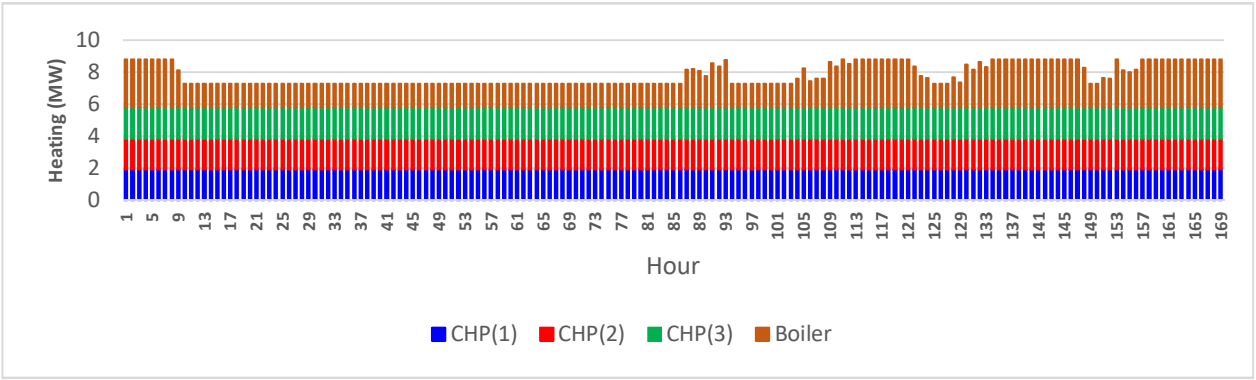

(a)

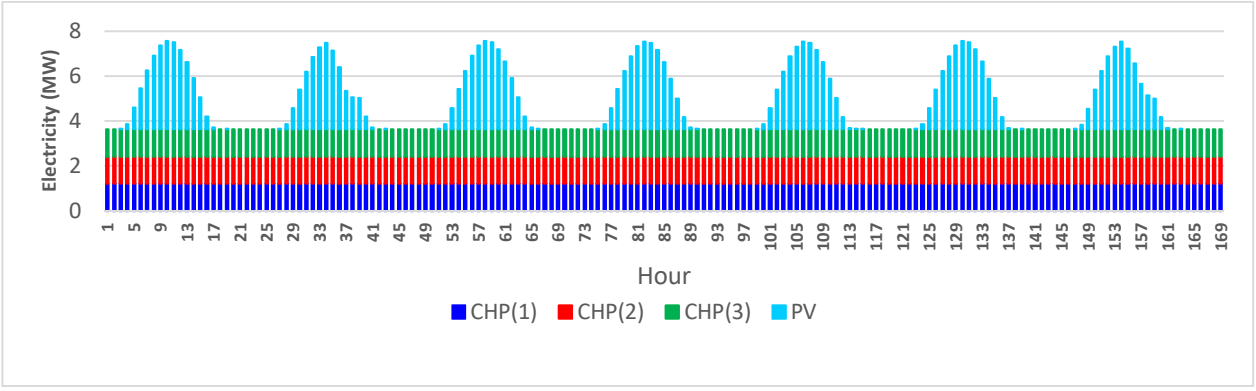

(b)

Fig.16. (a) The stacked column of the estimated values of the 5th zone optimal heating dispatch for the 5th scenario and the second week of June 2023. (b) The stacked column of the estimated values of the 5th zone optimal electricity dispatch for the 5th scenario and the second week of June 2023.

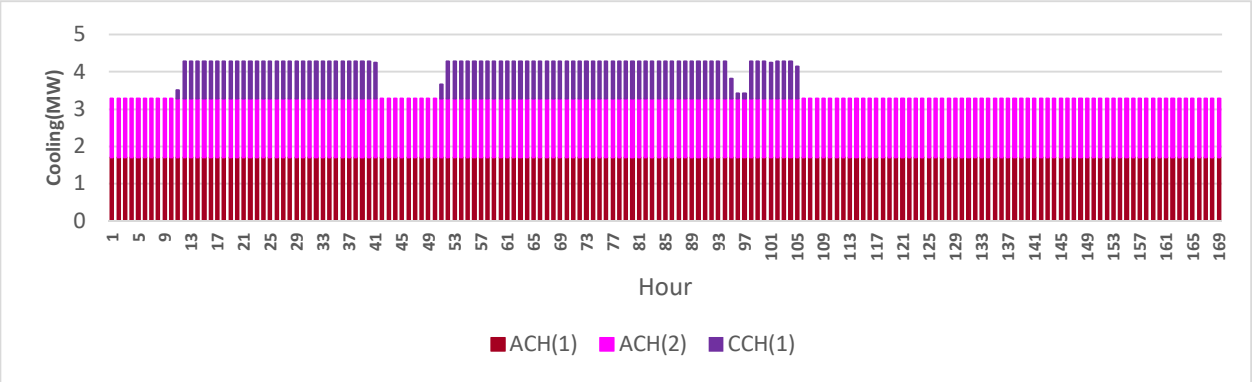

(a)

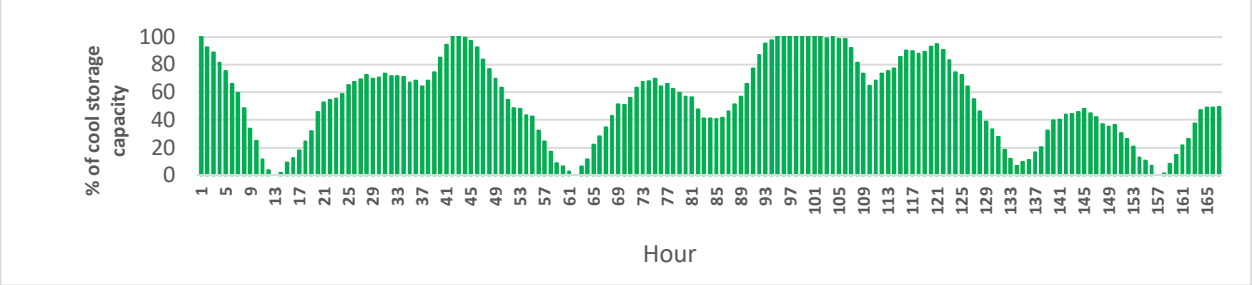

(b)

Fig. 17. (a) The stacked column of the estimated values of the 5th zone optimal cooling dispatch for the 5th scenario and the first week of June 2023. (b) The 5th zone optimal cooling storage charge and discharge for the 5th scenario and the first week of June 2023.

Fig. 18 (a) and (b) show the estimated values of the 2nd zone SWTs electricity generation and electricity storage charge and discharge for the 5th scenario and the third week of June 2023, respectively. The maximum value of battery storage was about 0.425 MWh.

As shown in Fig. 18 (a), the electricity generation of SWT is very low with respect to the electricity generation of other DERs.

As shown in Fig. 18 (b), the ESS was charged and discharged in a cyclic way based on the predefined State of Charge (SOC) thresholds. At each simulation interval of the second stage optimization problem (1 hour), the SOC of ESSs were checked. The ESS was charged in order to be in a position to accommodate the critical loads in contingency conditions for the next simulation step.

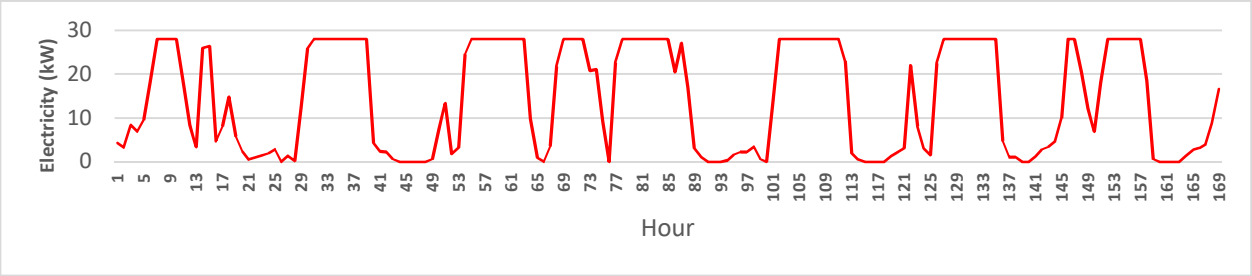

(a)

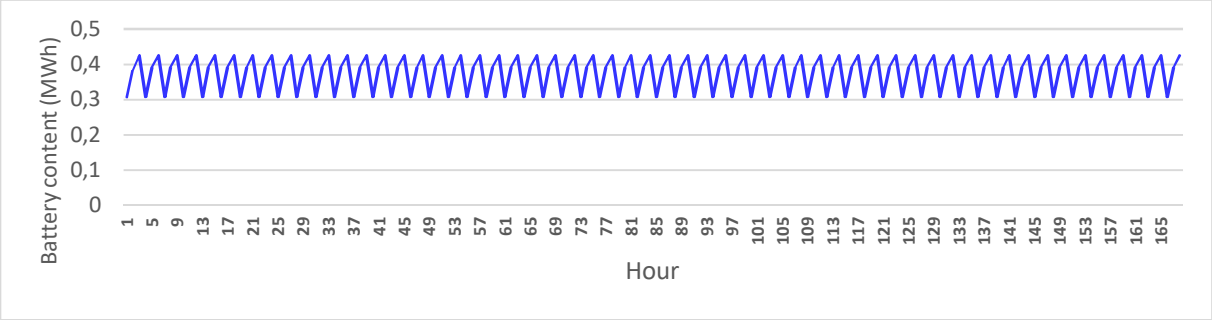

(b)

Fig. 18. (a) The estimated values of the 2nd zone SWTs electricity generation for the 5th scenario and the third week of June 2023. (b) The estimated values of the 2nd zone electricity storage charge and discharge for the 5th scenario and the third week of June 2023.

Fig. 19 (a), (b), (c), (d) and (e) depict the estimated values of electric load, electricity generation, import and export for the 4th scenario and zones and second week of January 2023, respectively. For the 1st, 4th and 5th zones, the CHPs were fully loaded when they were on; meanwhile, the 2nd zone CHP was fully committed. For all of the zones, the zonal exported electricity was delivered to the upward utility when the generated electricity was more than electricity consumption.

Fig. 20 shows the estimated values of aggregated electric load, electricity generation, import and export of AMG for the 4th scenario and the second week of January 2023. The ability of electricity export highly depends on the PVAs electricity generation. The AMG imports electricity when the PVAs were not available and the electricity generation of CHPs was less than its electricity consumption.

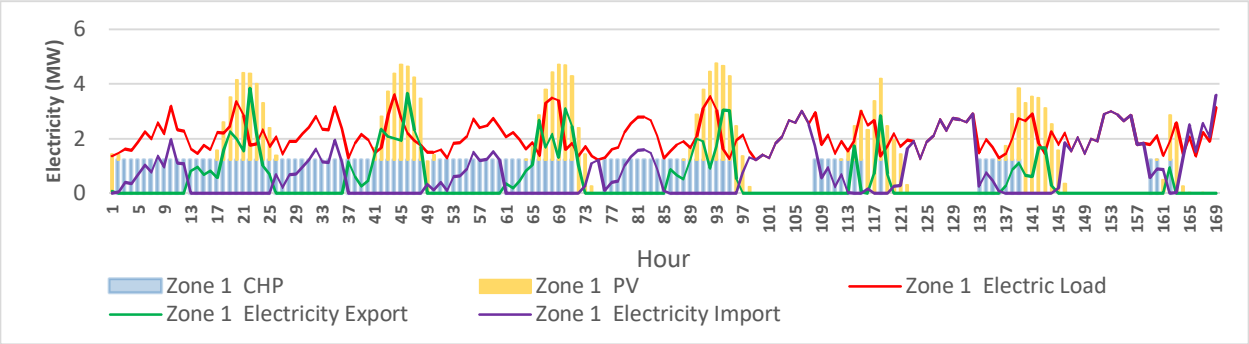
Electricity (MW)
Hour
Zone 1 CHP
Zone 1 PV
Zone 1 Electric Load
Zone 1 Electricity Export
Zone 1 Electricity Import

(a)

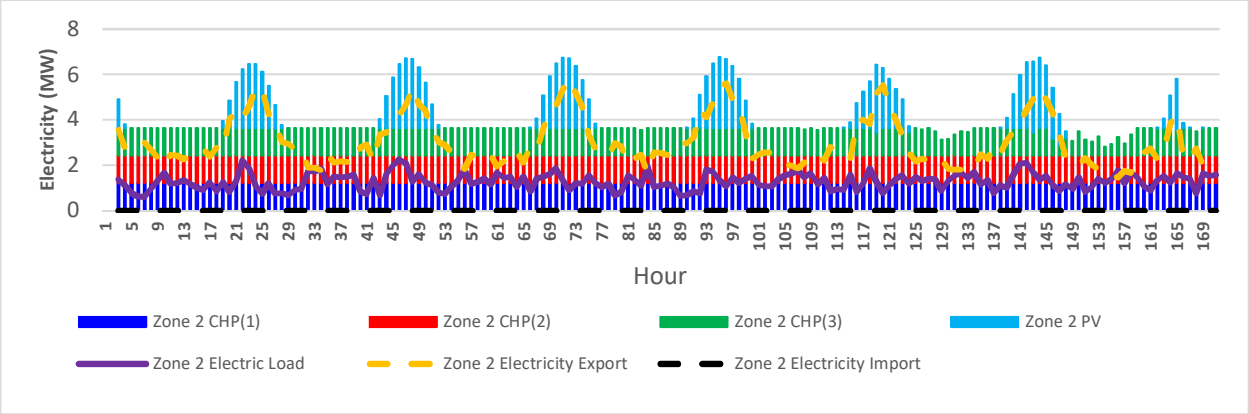
Electricity (MW)
Hour
Zone 2 CHP(1)
Zone 2 CHP(2)
Zone 2 CHP(3)
Zone 2 PV
Zone 2 Electric Load
Zone 2 Electricity Export
Zone 2 Electricity Import

(b)

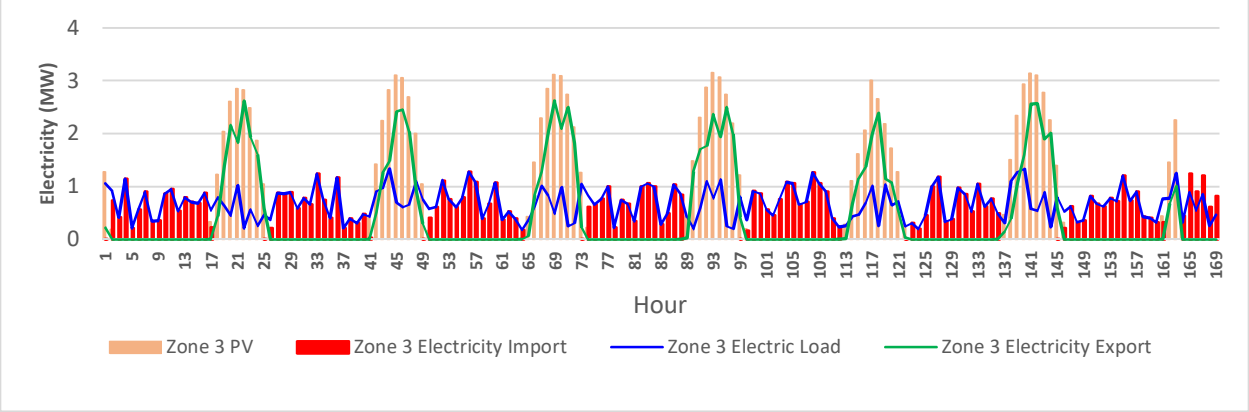
Electricity (MW)
Hour
Zone 3 PV
Zone 3 Electricity Import
Zone 3 Electric Load
Zone 3 Electricity Export

(c)

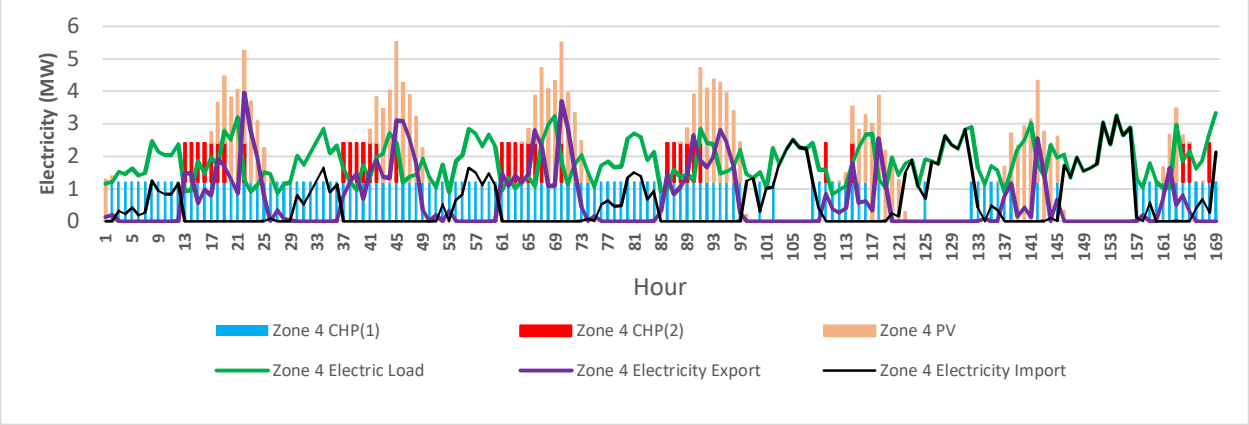
Electricity (MW)
Hour
Zone 4 CHP(1)
Zone 4 CHP(2)
Zone 4 PV
Zone 4 Electric Load
Zone 4 Electricity Export
Zone 4 Electricity Import

(d)

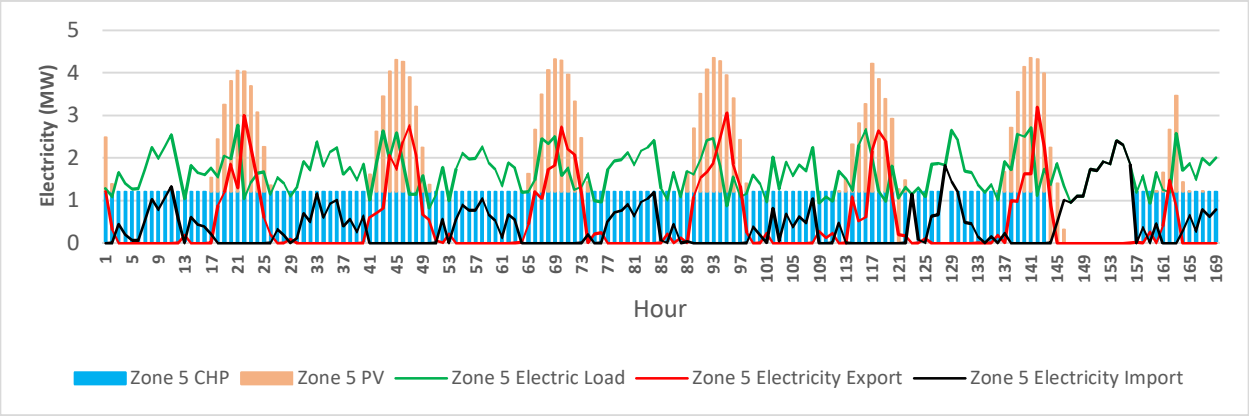

(e)

Fig. 19. The estimated values of electric load, electricity generation, import and export for the 4th scenario and second week of January 2023 and for (a) 1st zone, (b) 2nd zone, (c) 3rd zone, (d) 4th zone, (e) 5th zone.

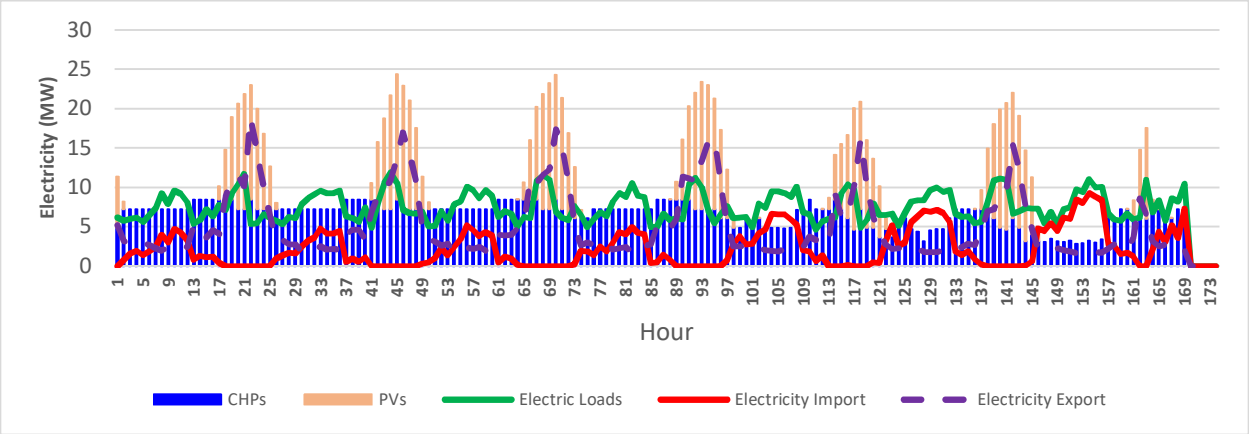

Fig. 20. The estimated values of aggregated electric load, electricity generation, import and export of AMG for the 4th scenario and second week of January 2023.

The DERNEP optimized the value of purchasing and selling electricity for different scenarios and operational condition. The surplus electricity energy of each site is delivered to the upward utility for the 5th scenario based on the fact that the electricity export price is about 125 percent of the electricity import price and the export of AMG electricity surplus to the upward network is quite economical.

Fig. 21 (a), (b), (c), (d) and (e) depict the estimated electric load, electricity generation, import and export for the 5th scenario and 1st, 2nd, 3rd, 4th and 5th zone and second week of January 2023, respectively.

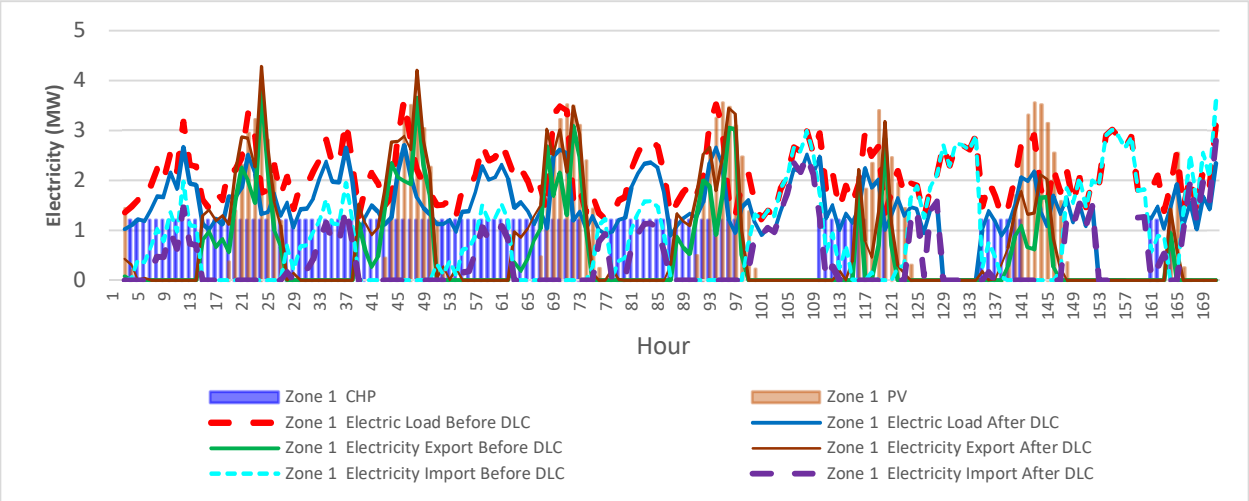
Electricity (MW)
Hour
Zone 1 CHP
Zone 1 PV
Zone 1 Electric Load Before DLC
Zone 1 Electric Load After DLC
Zone 1 Electricity Export Before DLC
Zone 1 Electricity Export After DLC
Zone 1 Electricity Import Before DLC
Zone 1 Electricity Import After DLC

(a)

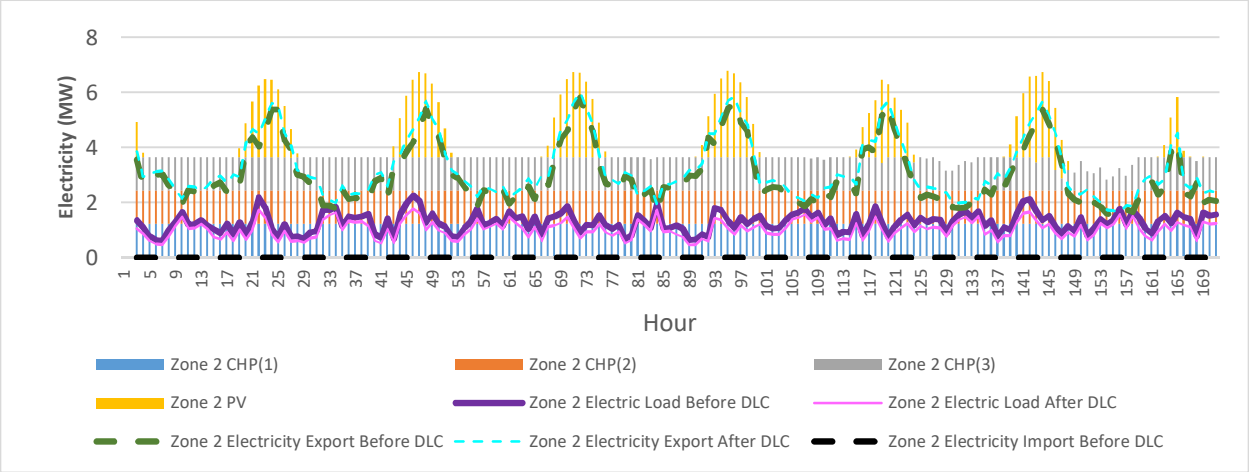
Electricity (MW)
Hour
Zone 2 CHP(1)
Zone 2 CHP(2)
Zone 2 CHP(3)
Zone 2 PV
Zone 2 Electric Load Before DLC
Zone 2 Electric Load After DLC
Zone 2 Electricity Export Before DLC
Zone 2 Electricity Export After DLC
Zone 2 Electricity Import Before DLC

(b)

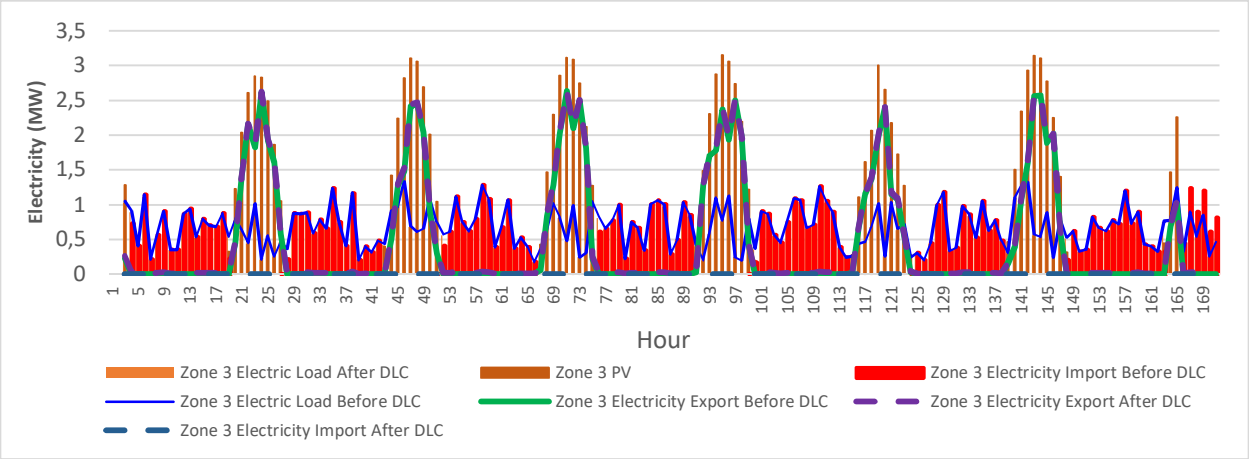
Electricity (MW)
Hour
Zone 3 Electric Load After DLC
Zone 3 PV
Zone 3 Electricity Import Before DLC
Zone 3 Electric Load Before DLC
Zone 3 Electricity Export Before DLC
Zone 3 Electricity Export After DLC
Zone 3 Electricity Import After DLC

(c)

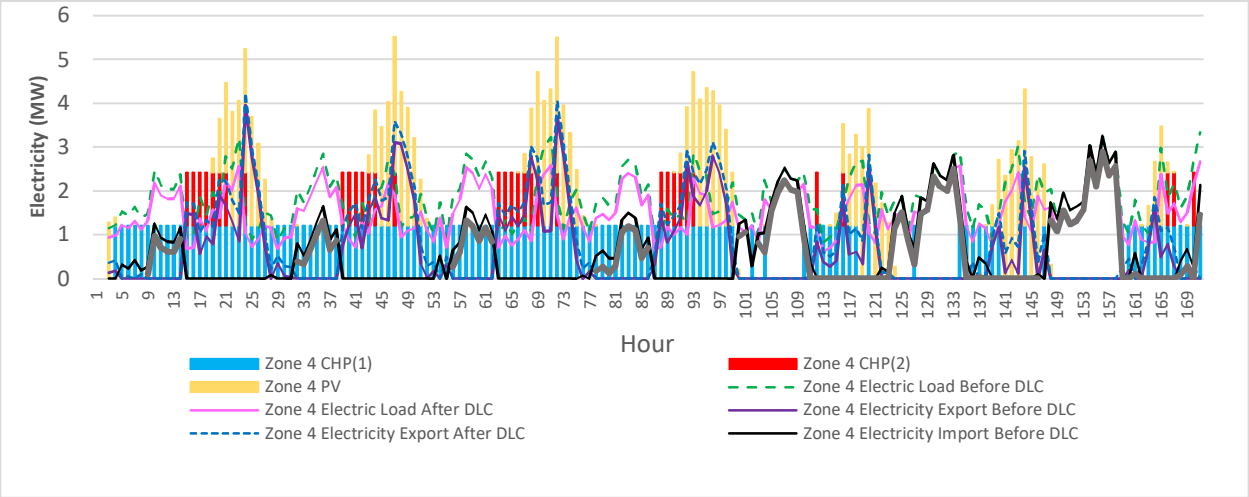

(d)

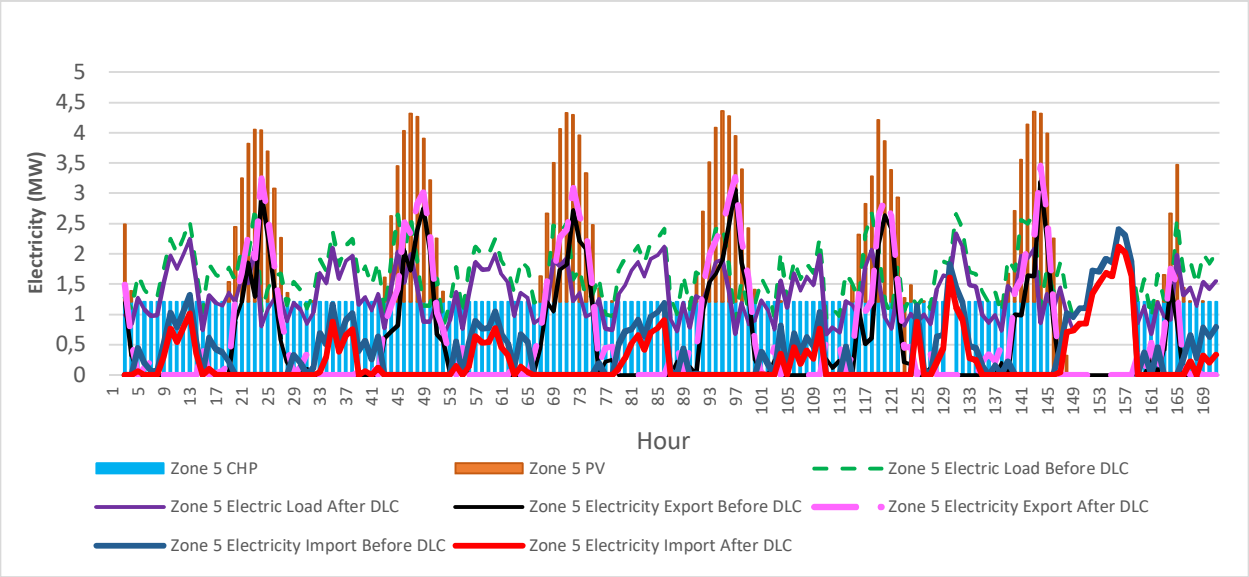

(e)

Fig. 21. The estimated electric load, electricity generation, import and export for the 5th scenario and second week of January 2023 and for: (a) 1st zone, (b) 2nd zone, (c) 3rd zone, (d) 4th zone, (e) 5th zone.

The ability of electricity export was highly improved after DLC implementation. Each zone imported less electricity when the DLC procedure was implemented and the electricity generation of zones was reduced.

Fig. 22 shows the estimated aggregated electric load, electricity generation, import and export of AMG for the 5th scenario and the second week of January 2023. The electricity export of the AMG was highly increased after DLC implementation and the AMG imported less electricity when the DLC procedure was implemented and the total electricity generation of CHPs was reduced.

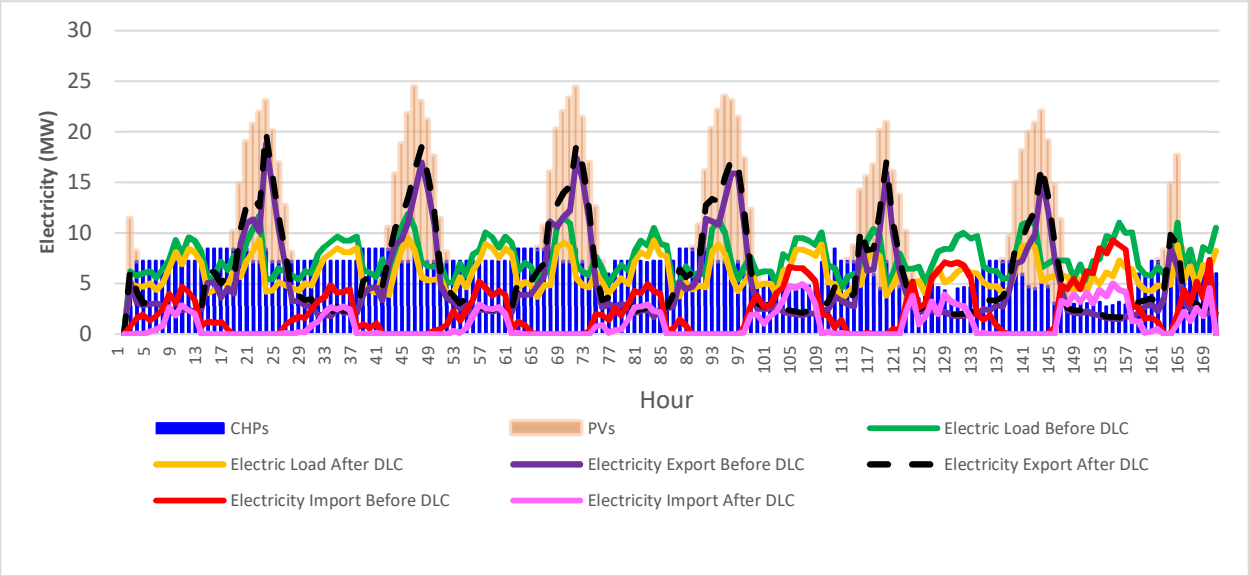

Fig. 22. The estimated aggregated electric load, electricity generation, import and export of AMG for the 5th scenario and second week of January 2023.

Fig. 23 depicts the estimated values of different AMG zones electricity import and export and natural gas consumption for the 2nd and 3rd scenarios at the horizon year. The electricity surplus export is highly dependent on the photovoltaic system and the natural gas consumption is reduced.

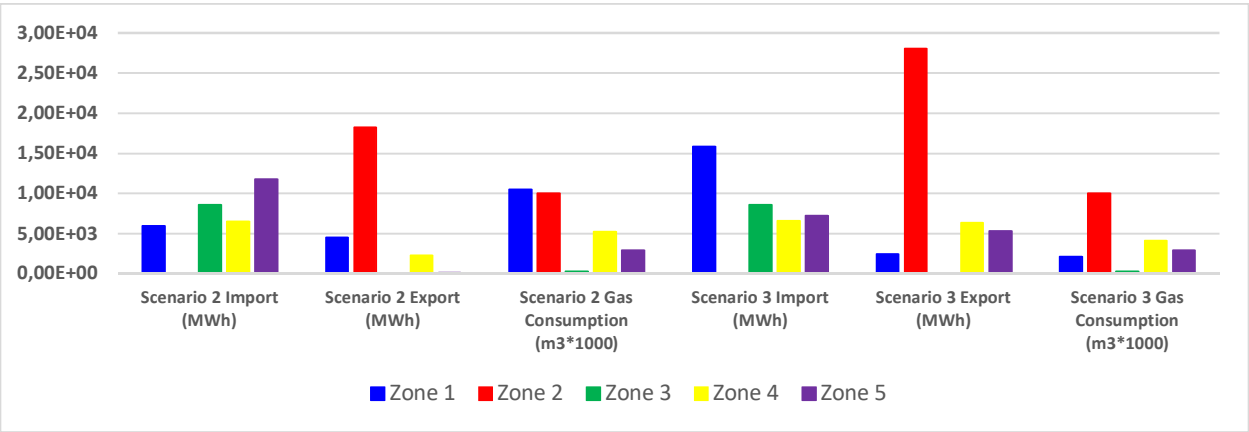

Fig. 23. The electricity import and export and natural gas consumption for the 2nd and 3rd scenarios and horizon year.

Fig. 24 shows the estimated electricity import and export for the 4th and 5th scenarios and horizon year. The surplus electricity of zones is exported to the upward utility at the TOU2 period when the photovoltaic systems generate electricity more than total electricity consumption. Further, the electricity import of the 2nd zone is zero for all scenarios.

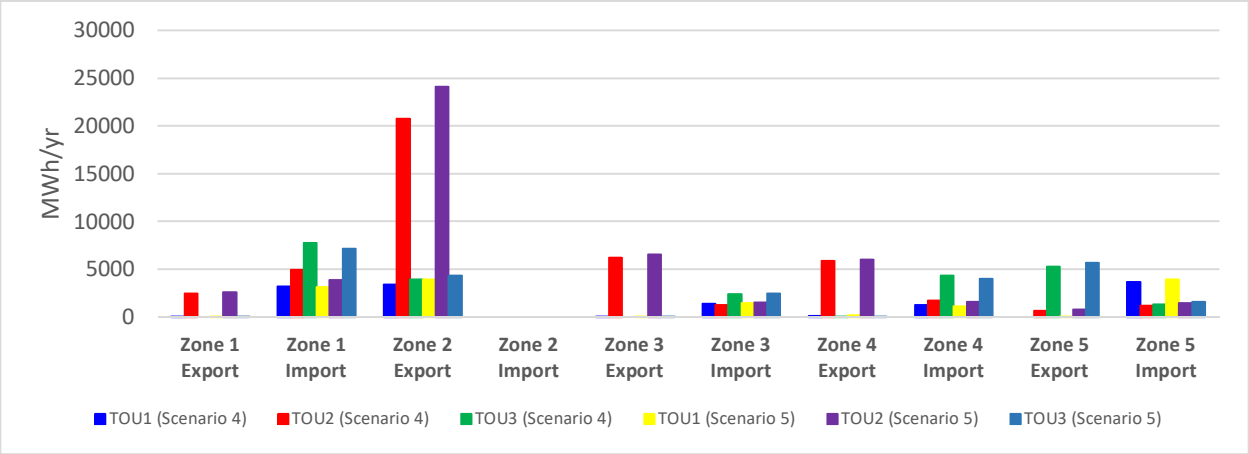

Fig. 24. The estimated electricity import and export for the 4th and 5th scenarios and horizon year.

Fig. 25 depicts the final investment, electricity and natural gas purchasing, emission and operational costs for different scenarios at the horizon year of planning.

According to Fig. 25, the implementation of DERNEP alternatives reduces the aggregated investment and operational costs of the system for the 4th and 5th scenario about 43.73% and 54.7% with respect to the 1st scenario costs, respectively. The AMG can sell its surplus electricity to the upward utility and the benefit of energy sold to the upward utility are about 3.86E+11 and 4.28E+11 MUs/yr. for the 4th and 5th scenario, respectively. Further, the 20 years operational costs are about -2.04E+9 and -1.5E+11 (MUs) for the 4th and 5th scenarios, respectively. It means that the AMG can gain benefit by participating in the upward utility's DRPs.

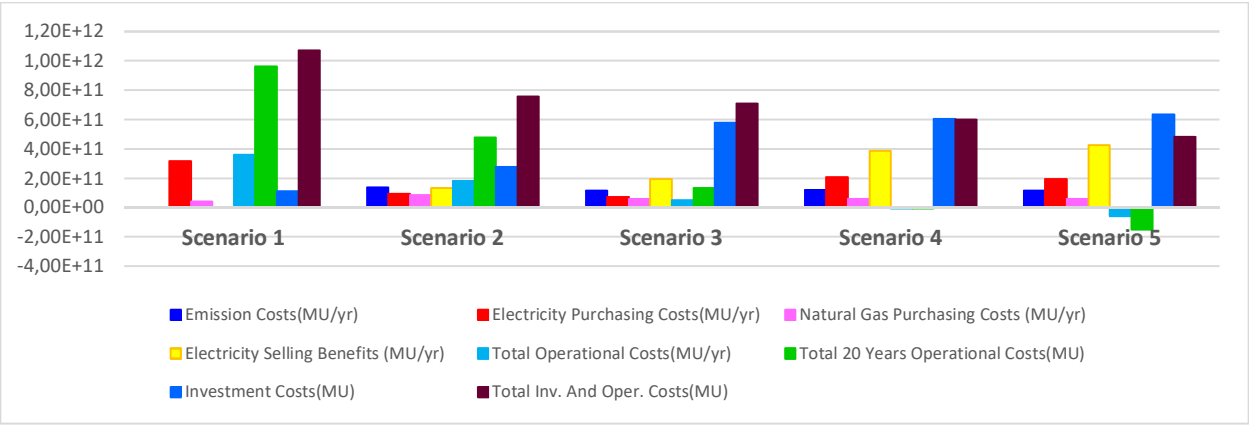

Fig. 25. The investment and operational costs scenarios at the horizon year.

A sensitivity analysis was carried out for the 5th scenario of the 2nd zone by changing the interruption cost parameter, starting from Table 4 values. Table 7 depicts the optimal DERNEP outputs consist of the optimal allocation, capacity and equipment characteristics for different values of the interruption costs.

Table 7. Sensitivity analysis results.

Interruption costs multiplied by	0.01	0.01	1	1	2.5	2.5	5	5
Year of Expansion planning	1	5	1	5	1	5	1	5
CHPs (kW)								
Zone 2	1×1210	1×1210	2×1210	3×1210	2×1210	3×1210	2×1210	3×1210
Boilers (kW)								
Zone 2	6000	6000	3000	3000	3000	3000	3000	3000
ACH (kW)								
Zone 2	1700	1700	1700	2×1700	1700	2×1700	1700	2×1700
CCH (kW)								
Zone 2	1000	2×1000	0	1000	0	1000	0	1000
PVA (kW)								
Zone 2	4000	4000	4000	4000	4000	4000	4000	4000
SWT (kW)								
Zone 2	8×3.5	8×3.5	8×3.5	8×3.5	18×3.5	30×3.5	32×3.5	56×3.5
ESS (kWh)								
Zone 2	1×100	1×100	5×100	5×100	10×100	12×100	25×100	40×100
CSS (MWh)								
Zone 2	4.55	4.55	12.75	12.75	12.75	12.75	12.75	12.75

As shown in Table 7, the installed capacity of CHPs, ACHs, ESSs, CSSs and SWTs were increased with the increase of the interruption costs; meanwhile, the installed capacity of CSSs was decreased. All of the available capacity of PVA panels were used based on the fact that the PVA panels were installed on the roof of the buildings.

Fig. 26 depict the fitness function variations over iterations for the 5th scenario.

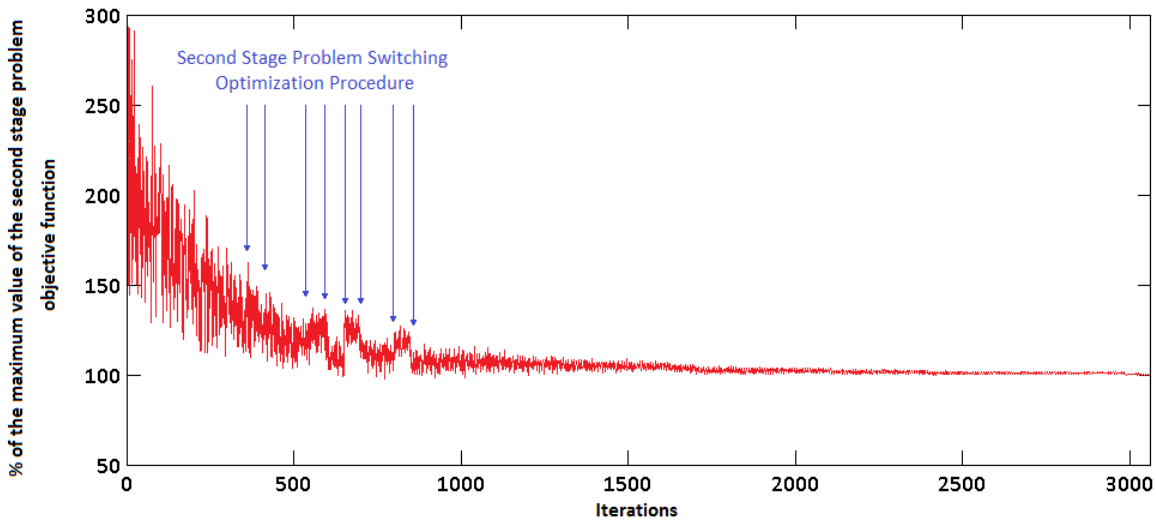

Fig. 26. The fitness function variations over iterations for the 5th scenario.

As shown in Fig. 26, the switching of the switching devices has changed the value of the objective function in contingent condition and finally, the problem can find the optimal resource coordination of system.

5. Conclusion

This paper addressed an integrated framework for DERNEP of an active microgrid that the energy resources were CHPs, small wind turbines, photovoltaic systems, electric and cooling storage, and gas-fired boilers and absorption and compression chillers. The conclusion can be summarized as follows:

(1) The proposed algorithm utilized a MINLP model to minimize investment, operational and emission cost; meanwhile, maximizing the system's reliability. The dynamic coupling constraints of cooling, heating and electric systems were taken into account in the proposed model.

(2) The proposed bi-level algorithm investigated the adequacy of system resources in the normal and contingent operational conditions. The optimization problem had a great non-convex discrete state space and the proposed solution algorithm had the ability to model the nonlinearity and non-convexity of the system's state space and the dynamic coupling constraints of the electric, heating and cooling systems.

(3) Five different scenarios were evaluated by different configurations and operational paradigms. Further, the upward utility DRPs were TOU and DLC programs that reduced electricity-purchasing costs. The final proposed layout of the system enabled the active microgrid to sell its surplus electricity to the upward utility and the benefit of energy sold to the upward utility was more than its operational costs.

(4) The implementation of DERNEP alternatives reduced the aggregated investment and operational costs of the system for the 4th and 5th scenario about 43.73% and 54.7% with respect to the 1st scenario costs, respectively. The AMG could sell its surplus

electricity to the upward utility and the benefit of energy sold to the upward utility were about 3.86E+11 and 4.28E+11 MUs/yr. for the 4th and 5th scenario, respectively.

(5) The 20 years operational costs were about -2.04E+9 (MUs) and -1.5E+11 (MUs) for the 4th and 5th scenarios, respectively. In conclusion, the adoption of the proposed DERNEP includes DERs allows increasing significantly the microgrid benefits and the reliability. The authors are investigating the use of other DERs, such as electric vehicles, for providing more DRP alternatives for the DERNEP procedure.

Acknowledgment

J.P.S. Catalão acknowledges the support by FEDER funds through COMPETE 2020 and by Portuguese funds through FCT, under Projects SAICT-PAC/0004/2015 - POCI-01-0145-FEDER-016434, POCI-01-0145-FEDER-006961, UID/EEA/50014/2013, UID/CEC/50021/2013, UID/EMS/00151/2013, and 02/SAICT/2017 - POCI-01-0145-FEDER-029803.

References

1- Wei Gu, Zhi Wub, Rui Bo, Wei Liu, Gan Zhou, Wu Chen, Zaijun Wu, Modeling," Planning and optimal energy management of combined cooling, heating and power microgrid: A review", *Electr. Power Energy Syst.*, 2014, **54**, pp. 26–37.

2- S. Chowdhury, S.P. Chowdhury and P. Crossley, "Microgrids and active distribution networks", The institution of engineering and technology, 2009.

3- Aringhieri R, Malucelli F., "Optimal operations management and network planning of a district system with a combined heat and power plant". *Annals of Operations Research,* 2003,**120**, pp.173–199.

4- Chicco G, Mancarella P., "Distributed multi-generation: a comprehensive view", *Renew. Sustain. Energy Revs.*, 2009, **13**, pp. 535–551.

5- Gopalakrishnan H., Kosanovic D., "Economic optimization of combined cycle district heating systems," *Sustainable Energy Technologies and Assessments*, 2014, **7**, pp. 91-100.

6- Salgado F., Pedrero P., "Short-term operation planning on cogeneration systems: A survey," *Electr. Power Syst. Res.*, 2008, **78**, (5), pp. 835-848.

7- Lozano M, Ramos J, Serra L., "Cost optimization of the design of CHCP (combined heat, cooling and power) systems under legal constraints", *Energy*, 2010, **35**, pp. 794–805.

8- Carvalho M, Serra LM, Lozano MA. "Optimal synthesis of tri-generation systems subject to environmental constraints", *Energy*, 2011, **36**, pp. 3779–3790.

9- Xuyue Zheng, Guoce Wu, Yuwei Qiu, Xiangyan Zhan, Nilay Shah, Ning Li, Yingru Zhao, "A MINLP multi-objective optimization model for operational planning of a case study CCHP system in urban China", *Appl. Energy*, 2018, **210**, pp. 1126-1140.

10- Zelin Li, Qingsong An, Jun Zhao, Shuai Deng, Ligai Kang, Yongzhen Wang, "Analysis of system optimization for CCHP system with different feed-in tariff policies", *Energy Procedia*, 2017, **105**, pp. 2484 – 2491.

11- Miao Li, Hailin Mu, Nan Li, Baoyu Ma, "Optimal design and operation strategy for integrated evaluation of CCHP (combined cooling heating and power) system", *Energy*, 2016, **99**, pp. 202-220.

12- Liwei Ju, Zhongfu Tan, Huanhuan Li, Qingkun Tan, Xiaobao Yu, Xiaohua Song, "Multi-objective operation optimization and evaluation model for CCHP and renewable energy based hybrid energy system driven by distributed energy resources in China", *Energy*, 2016, **111**, pp. 322-340.
13- Sakawa M, Kato K, Ushiro S., "Operational planning of district heating and cooling plants through genetic algorithms for mixed linear programming", *J. Oper. Res.*, 2002, **137**, pp. 677–687.
14- Weber C, Shah N., "Optimization based design of a district energy system for an eco-town in the united kingdom", *Energy*, 2011, **36**, pp.1292–1308.
15- M. Ameri, Z.Besharati, "Optimal design and operation of district heating and cooling networks with CCHP systems in a residential complex", *Energy and Buildings*, 2016, (1), **110**, pp. 135-148.
16- Soderman J, Petterson F., "Structural and operational optimization of distributed energy systems", *Appl. Thermal Engineering*, 2006, **26**, pp. 1400–1408.
17- Mehleri ED, Sarimveis H, Markatos NC, Papageorgiou LG, "Optimal design and operation of distributed energy systems: application to Greek residential sector", *Renew. Energy*, 2013, **51**, pp. 331–342.
18- Bracco S, Gabriele D, and Silvia S., "Economic and environmental optimization model for the design and the operation of a combined heat and power distributed generation system in an urban area", *Energy*, 2013, 55, pp. 1014–1024.
19- Mohammad Hadi Shaban Boloukat, Asghar Akbari Foroud, "Stochastic-based resource expansion planning for a grid-connected microgrid using interval linear programming", *Energy,* **113**, pp. 776-787, 2016.
20- Reza Hemmati, Hedayat Saboori, Pierluigi Siano, "Coordinated short-term scheduling and long-term expansion planning in microgrids incorporating renewable energy resources and energy storage systems", *Energy,* **134**, pp. 699-708, 2017.
21- Yokoyama, Ryohei, Yasushi Hasegawa, and Koichi Ito. "A MILP decomposition approach to large scale optimization in structural design of energy supply systems." *Energy Convers. Manage.*, 2002, **43**, (6), pp. 771-790.
22- M. Setayesh Nazar, M.R. Haghifam, M. Nazar, "A scenario driven multiobjective Primary–Secondary Distribution System Expansion Planning algorithm in the presence of wholesale–retail market", *Int. J. Electr. Power Energy Syst*., **40**, pp. 29–45, Sep. 2012.
23- S. Ashok, R. Banerjee, "Optimal cooling storage capacity for load management", *Energy*, 2003, **28**, pp. 115–126.
24- Mohsen Kia, Mehrdad Setayesh Nazar, Mohammad Sadegh Sepasian, Alireza Heidari, and João P. S. Catalão, "New framework for optimal scheduling of combined heat and power with electric and thermal storage systems considering industrial customers inter-zonal power exchanges", *Energy*, 2017, **138**, (1), pp. 1006-1015.
25- Jun, Z., Junfeng, L., Jie, W., Ngan, H.W., "A multi-agent solution to energy management in hybrid renewable energy generation system", *Renew. Energy*, 2011, **36**, 1, pp. 1352–1363.
26- David Wood, "Small wind turbines, Analysis, design, and application", Springer-Verlag book company, 2011.
27- D. T. Nguyen, and L. B. Le, "Optimal Bidding Strategy for Microgrids Considering Renewable Energy and Building Thermal Dynamics", IEEE Trans. Smart Grid, 2014, **5**, no. 4, pp. 1608-1620.
28- Mohsen Kia, Mehrdad Setayesh Nazar, Mohammad Sadegh Sepasian, Alireza Heidari, Pierluigi Siano, "An efficient linear model for optimal day ahead scheduling of CHP units in active distribution networks considering load commitment programs". ", *Energy*, 2017, **139**, pp. 798-817.
29- Solar turbines data sheet, URL: https://mysolar.cat.com
30- Sanaye S, Khakpaay N. Simultaneous use of MRM (maximum rectangle method) and optimization methods in determining nominal capacity of gas engines in CCHP (combined cooling, heating and power) systems. *Energy* 2014, **72**, pp. 145–58.
31- Wind turbine data sheets, URL:http://usa.windspot.es/home-wind-turbines/products/89/windspot-35-kw/
32- Photovoltaic costs and prices sheets, URL:https://www.nrel.gov/docs/fy15osti/64746.pdf
33- Chillers data sheets, URL:www.carrier.com/commercial/en/us/products/chillers-components/chillers

34- Wang Jiang-Jiang, Zhang Chun-Fa, Jing You-Yin, Zheng Guo-Zhong, "Using the fuzzy multi-criteria model to select the optimal cooling storage system for air conditioning", *Energy and Buildings*, 2008, **40**, pp. 2059–2066.
35- Casisi, M., P. Pinamonti, and M. Reini. Optimal lay-out and operation of combined heat & power (CHP) distributed generation systems. Energy 2009, 34, pp. 2175–2183.
36- Solar irradiation data, URL: http://solarchvision.com
37- Metrological data sheets, URL: http://irimo.ir/eng